INHIBITION OF CEREBELLAR DYSFUNCTION IN MANGANESE CHLORIDE-EXPOSED WISTAR RATS TREATED WITH VANILLIN

BY

OBOH-VINCENT CHELSEA EFEZINO
BMS2101343

SUPERVISOR:

DR. A. B. ENOGIERU

DEPARTMENT OF ANATOMY
SCHOOL OF BASIC MEDICAL SCIENCES
COLLEGE OF MEDICAL SCIENCES

UNIVERSITY OF BENIN

NOVEMBER, 2025.

INHIBITION OF CEREBELLAR DYSFUNCTION IN MANGANESE CHLORIDE-EXPOSED WISTAR RATS TREATED WITH VANILLIN

BY

OBOH-VINCENT CHELSEA EFEZINO
BMS2101343

A PROJECT SUBMITTED TO THE DEPARTMENT OF ANATOMY, SCHOOL OF BASIC MEDICAL SCIENCES, COLLEGE OF MEDICAL SCIENCES, UNIVERSITY OF BENIN, BENIN CITY.

IN PARTIAL FULFILLMENT FOR THE AWARD OF BACHELOR OF SCIENCE (BSc.) DEGREE IN ANATOMY OF THE UNIVERSITY OF BENIN, BENIN CITY

NOVEMBER, 2025

DECLARATION

I declare that:

1. This project report is based on the experimental work undertaken by me in the Department of Anatomy, University of Benin, under the supervision of Dr. Adaze B. Enogieru.
2. This work has not been previously submitted for the award of a degree elsewhere.
3. All ideas and views are essentially based on this research. And where the views of others have been expressed, such words were duly acknowledged.

_____

OBOH-VINCENT CHELSEA EFEZINO

BMS2101343

CERTIFICATION

This is to certify that this project work titled "**INHIBITION OF CEREBELLAR DYSFUNCTION IN MANGANESE CHLORIDE-EXPOSED WISTAR RATS TREATED WITH VANILLIN**" was carried out by **OBOH-VINCENT CHELSEA EFEZINO** in the Department of Anatomy, School of Basic Medical Sciences, University of Benin, Benin City, Nigeria.

_____ _____

ADAZE B. ENOGIERU (PhD) **DATE**

Supervisor

_____ _____

ADAZE B. ENOGIERU (PhD) **DATE**

Head of Department

_____ _____

EXTERNAL EXAMINER **DATE**

DEDICATION

I dedicate this project to GOD Almighty, whose grace and wisdom have guided me through every step of this journey. Without him, I wouldn't have made it this far.

ACKNOWLEDGEMENT

I express my profound gratitude to my supervisor DR. ADAZE B. ENOGIERU, for his continuous guidance, patience, encouragement and support throughout the course of this research. His mentorship has been truly inspiring, and working under his supervision has been one of the most rewarding experiences of my academic journey. My heartfelt appreciation also goes to my dearest parents, Mr. and Mrs. Oboh, whose endless support, sacrifices and prayers have been the foundation of all my achievements.

To my boyfriend, Clinton, thank you for being my biggest cheerleader. Your love and support gave me the strength to keep pushing forward, and I couldn't have done this without you. To my amazing friends and research partners, Monalisa and Natasha, thank you for being such a beautiful part of this journey, I deeply appreciate their dedication, teamwork, laughter and support throughout this project. The memories we created will always hold a special place in my heart. Finally, I extend my gratitude to the Head of department, professors, lecturers and laboratory staff of the Department of Anatomy, University of Benin. For providing the facilities that made this entire research possible.

TABLE OF CONTENTS

TITLE PAGE i
DECLARATION ii
CERTIFICATION iii
ACKNOWLEDGEMENT v
TABLE OF CONTENTS vi
CHAPTER ONE 1
INTRODUCTION 1
1.1 BACKGROUND OF THE STUDY 1
1.2 STATEMENT OF RESEARCH PROBLEM 2
1.3 AIM OF THE STUDY 3
1.4 SPECIFIC OBJECTIVES OF THE STUDY 3
1.5 JUSTIFICATION OF THE STUDY 4
CHAPTER TWO 6
LITERATURE REVIEW 6
2.1 MANGANESE CHLORIDE ($MnCl_2$) 6
2.1.1 Characteristics and Uses 6
2.1.2 Toxicokinetics 7
2.1.3 Neurotoxic Effects of Manganese 11
2.2 VANILLIN 15
2.2.1 Sources of Vanillin 16
2.2.2 Bioactivities 17
2.3 THE CEREBELLUM 28
2.3.1 Cytoarchitecture of the Cerebellum 30
2.3.2 Connections of the Cerebellum 32
2.3.3 Functions of the Cerebellum 34
2.3.4 Arterial Supply of the Cerebellum 35
2.3.5 Venous Drainage of the Cerebellum 36
CHAPTER THREE 37
MATERIALS AND METHODS 37
3.1 REAGENT / CHEMICALS 37
3.2 EQUIPMENT 37
3.3 EXPERIMENTAL ANIMALS 37
3.4 RESEARCH DESIGN 38

3.5 NEUROBEHAVIOURAL ASSESSMENTS 38
3.5.1 Open Field Test 38
3.5.2 String Test 39
3.5.3 Movement Initiation Test 39
3.5.4 Step Test 40
3.6 EVALUATION OF BRAIN WEIGHT 40
3.7 CEREBELLAR OXIDATIVE STRESS PARAMETERS 40
3.7.1 Estimation of Catalase (CAT) activity 41
3.7.2 Estimation of Malondialdehyde (MDA) activity 41
3.7.3 Estimation of Glutathione Peroxidase (GPx) activity 42
3.7.4 Estimation of Superoxide Dismutase (SOD) 43
3.8 HISTOLOGY OF THE CEREBELLUM 44
3.9 HEMATOXYLIN AND EOSIN STAINING PROCEDURES 44
3.10 PHOTOMICROGRAPHY 45
3.11 STATISTICAL ANALYSIS 45
CHAPTER FOUR 46
RESULTS 46
4.1 Effects of Treatment on Body and Brain Weight 46
4.2 Effects of Treatment on Neurobehavioural Activity 50
4.2.1 Open Field Test 50
4.2.2 String Test 53
4.2.4 Step Test 55
4.3 Effects of Treatment on Oxidative Stress 56
4.4 Effects of Treatment on Histology 59
CHAPTER FIVE 63
DISCUSSION, CONCLUSION AND RECOMMENDATION 63
5.1 DISCUSSION 63
5.2 CONCLUSION 67
5.3 RECOMMENDATION 67
REFERENCES 68

ABSTRACT

Cerebellar dysfunction, marked by impaired coordination and balance, often result from toxic or degenerative damage to cerebellar neurons. Excessive exposure to manganese chloride, a neurotoxic compound, disrupts neuronal integrity through oxidative stress and inflammation, leading to motor and structural deficits. Vanillin, a natural phenolic compound with strong antioxidant and anti-inflammatory properties, has shown potential in mitigating such neurotoxic effects. This study therefore investigated the protective effect of vanillin against manganese chloride–induced cerebellar toxicity in Wistar rats. Forty-eight (48) Wistar rats were randomly assigned into six groups (A-F). Group A rats served as the control group; Group B rats were administered 10 mg/kg body weight of manganese chloride; Group C rats were administered 20 mg/kg body weight of vanillin and 10 mg/kg body weight of manganese chloride; Group D was administered 40 mg/kg body weight of manganese chloride and 40 mg/kg body weight of vanillin; Group E was administered 20 mg/kg body weight of vanillin; Group F was given 40 mg/kg body weight of vanillin. All administrations lasted for twenty-eight (28) days. Neurobehavioural activities were evaluated using the open field, movement initiation, step and string Tests. Results from the study revealed that rats exposed to manganese chloride exhibited significant ($p<0.05$) weight loss, motor deficit, impaired antioxidant defense, elevated lipid peroxidation and degeneration of Purkinje cells and molecular layer neurons. However, pre-treatment with Vanillin significantly ($p<0.05$) mitigated these manganese chloride-induced cerebellar alterations in Wistar rats. Overall, the findings from this study indicate that vanillin possesses strong antioxidant properties, supporting its potential as an effective therapeutic agent for the treatment and management of manganese chloride-induced cerebellar dysfunction.

CHAPTER ONE

INTRODUCTION

1.1 BACKGROUND OF THE STUDY

The nervous system consists of the brain, spinal cord, and an extensive network of nerves that coordinate and regulate major functions of the body (Sabina *et al*., 2024). This highly specialized system integrates neuronal processes, neurotransmitters, and receptors to control movement, cognition, vision, balance, speech, cardiac activity, respiration, and other essential physiological functions (Banerjee *et al*., 2023; Sabina *et al*., 2024). However, the nervous system is highly susceptible to toxic injury, with the brain being the most vulnerable target (Wei and Guan, 2021). Various toxicants, including heavy metals such as manganese (Mn), are recognized as neurotoxins due to their capacity to disrupt neuronal integrity and impair normal brain function (Gurol *et al*., 2022). Exposure to such neurotoxicants may result in neurodegeneration, long-term neurological dysfunction, and in severe cases, death (Studer *et al*., 2022).

Manganese is an essential trace element involved in enzymatic functions and metabolic processes, but chronic overexposure leads to significant neurotoxicity (Obeng *et al*., 2024). Environmental and occupational exposure often occurs through contaminated air, water, food, and industrial activities such as mining, welding, and battery production (Gurol *et al*., 2022). Once absorbed, manganese crosses the blood-brain barrier and accumulates in vulnerable brain regions, including the basal ganglia and cerebellum (McCabe and Zhao, 2021). The cerebellum, which plays a central role in motor coordination, balance, and fine-tuned movement, is particularly sensitive to manganese-induced injury due to its high metabolic demand and dense neuronal circuitry (McCabe and Zhao, 2021). Manganese accumulation in the cerebellum leads to oxidative stress, mitochondrial dysfunction, and excitotoxicity, which together damage Purkinje cells and other neuronal populations, resulting in ataxia, tremors,

impaired coordination, and cognitive disturbances (Tarnacka *et al*., 2021; Katiyar *et al*., 2022). Chronic exposure has also been implicated in neurodegenerative disorders with Parkinsonian-like symptoms, a condition historically termed manganism (Tarnacka *et al*., 2021).

Since oxidative stress and neuroinflammation are key mechanisms of manganese toxicity, antioxidant-based therapeutic approaches have gained attention. Exogenous antioxidants counteract oxidative stress by scavenging free radicals, stabilizing cell membranes, and blocking lipid peroxidation pathways (Engwa *et al*., 2017). Natural products, particularly plant-derived compounds, are a major source of such antioxidants (Manessis *et al*., 2020). Medicinal plants have long been used in traditional medicine and are rich in bioactive phytochemicals with neuroprotective potential (Manessis *et al*., 2020). Among them, vanillin, a phenolic aldehyde and the principal component of vanilla bean extract has gained increasing attention. In addition to its wide use as a flavouring and fragrance agent, vanillin exhibits potent antioxidant (Scipioni *et al*., 2018), anti-inflammatory (Bezerra-Filho *et al*., 2019), and neuroprotective activities (Iannuzzi *et al*., 2023). Experimental studies have shown that vanillin mitigates oxidative stress, reduces pro-inflammatory cytokines, and protects neurons against excitotoxic and heavy metal-induced damage (Wang *et al*., 2025). These properties suggest that vanillin potentially may play an important role in attenuating manganese-induced cerebellar neurotoxicity.

1.2 STATEMENT OF RESEARCH PROBLEM

Despite the nervous system's compensatory and adaptive mechanisms, injuries to this system are largely irreversible due to the limited capacity of neurons to regenerate after initial development (Nagappan *et al*., 2020). Such injuries often result in permanent and debilitating loss of function (Nagappan *et al*., 2020). Neurotoxicity can arise from exposure to heavy metals, environmental contaminants, trauma, oxidative stress, and genetic abnormalities

(Ijomone *et al*., 2020). Environmental pollutants are considered major contributors to the development of neurotoxicity. These pollutants can be introduced into the environment through human activities such as mining, welding, battery production, and agricultural practices, which release excessive amounts of manganese into soil, water, and air (Dey *et al*., 2023; Sharifi *et al*., 2023).

The cerebellum, a brain region critical for motor coordination, balance, and cognitive processing, is particularly vulnerable to manganese toxicity due to its high metabolic demand and neuronal complexity (Tarnacka *et al*., 2021; Kulshreshtha *et al*., 2021). Elevated manganese levels in the cerebellum have been associated with motor dysfunctions such as tremors, ataxia, impaired coordination, and postural instability (Kulshreshtha *et al*., 2021). Furthermore, manganese accumulation disrupts neurotransmitter systems, induces oxidative stress, and damages Purkinje cells, leading to progressive cerebellar degeneration (Tarnacka *et al*., 2021). Studies have also linked early-life exposure to manganese with long-term behavioural deficits, reduced cognitive performance, and learning difficulties (Sanders *et al*., 2015; Lucchini *et al*., 2017). Despite increasing awareness of manganese neurotoxicity, there is currently no definitive treatment to reverse its effects on the cerebellum.

1.3 AIM OF THE STUDY

The aim of this study was to investigate the activity of vanillin on Manganese chloride-induced cerebellar toxicity in adult Wistar rats.

1.4 SPECIFIC OBJECTIVES OF THE STUDY

The specific objectives of the study are to investigate the activity of vanillin on:

i. the body and brain weight changes in rats treated with or without manganese chloride
ii. the neuro-behavioural activity (open field, string, movement initiation, and step tests) of rats treated with or without manganese chloride

iii. the antioxidant enzymes (superoxide dismutase, catalase, glutathione peroxidase) activity in the cerebellum of rats treated with or without manganese chloride.

iv. the lipid peroxidation (malondialdehyde concentration) in the cerebellum of rats treated with or without manganese chloride.

v. the histology of the cerebellum of rats treated with or without manganese chloride.

1.5 JUSTIFICATION OF THE STUDY

The use of orthodox drugs such as anticonvulsants (e.g., divalproex), tranquilizers (e.g., diazepam), and sedatives (e.g., zolpidem) for the management of neurological disorders is often accompanied by severe side effects, including swelling of the limbs, reduced heart rate, and chronic back pain (Srivastava *et al.*, 2019). Similarly, pharmacological treatment of Parkinsonism with drugs such as carbidopa and levodopa may lead to side effects including hallucinations, bladder pain, and chest pain (Mouchaileh and Hughes, 2020). Since most neurotoxic agents exert their harmful effects primarily through oxidative stress, antioxidants have been widely investigated for their ability to protect against such toxic insults (Olufunmilayo *et al*., 2023). Despite the protective role of endogenous antioxidants, supplementation with exogenous antioxidants has been shown to enhance the overall antioxidant defense system of the body and improve resilience against oxidative damage (Engwa *et al*., 2022).

Medicinal plants and natural compounds have been extensively reported to possess strong antioxidant properties (Nwozo *et al*., 2023). Because of their natural origin, affordability, accessibility, and minimal side effects, plant-derived compounds have attracted significant attention as alternative or complementary therapeutic agents in neuroprotection and drug discovery (Prakash and Verma, 2024). Vanillin, a phenolic aldehyde and the principal bioactive component of vanilla beans, has been shown to possess diverse pharmacological properties,

including antioxidant, anti-inflammatory, and neuroprotective activities (Arya *et al*., 2021; Iannuzzi *et al*., 2023; Kafali *et al*., 2024). Its ability to scavenge reactive oxygen species and suppress proinflammatory mediators highlights its potential as a therapeutic agent against neurodegenerative conditions linked to oxidative stress. Given that manganese-induced cerebellar toxicity is mediated largely through oxidative stress, mitochondrial dysfunction, and inflammation (Tarnacka *et al*., 2021), vanillin consequently provides neuroprotective potential against manganese-induced cerebellar damage.

CHAPTER TWO

LITERATURE REVIEW

2.1 MANGANESE CHLORIDE ($MnCl_2$)

2.1.1 Characteristics and Uses

Manganese (Mn) is a transition metal that has been known to humankind for centuries, with its scientific recognition and systematic description becoming more prominent during the 19th and early 20th centuries (Gurol *et al.*, 2022). However, archaeological evidence suggests that Mn compounds were employed as pigments by ancient civilizations, with traces found in cave paintings dating back over 17,000 years (Domingo and Chieli, 2021). As an element, Mn holds a significant position in the Earth's composition. It is not a rare or obscure metal, but rather one of the most plentiful in nature, ranking as the twelfth most abundant element in the Earth's crust and the fifth most abundant metal overall (Studer *et al.*, 2022). In its pure form, it presents as a silvery-gray metal with a subtle pinkish hue, a brittle and hard material that resists shaping at room temperature. It has a relatively high melting point of 1,246 °C and a density of about 7.21 g/cm³, reflecting its strong metallic bonding. Mn is highly reactive and readily combines with other nonmetals, demonstrating its ability to form diverse compounds, and this ability underpins its significance in catalysis, redox reactions, and even biological processes, where Mn acts as a vital cofactor in enzymes that sustain life (Gurol *et al.*, 2022).

As an abundant metal in nature, it is of great environmental and industrial relevance, in that, the metal and its compounds have been an important constituent of numerous manufacturing processes, including steel production, where it improves hardness, stiffness, corrosion resistance and strength, applications in the manufacture of dry-cell batteries, matches, fireworks, glass, and ceramics, paints, certain pesticides, leather and textile industries, and antiknock agent in gasoline; and in preparation of fertilizers, livestock nutritional supplements and animal feed (Sobańska *et al.*, 2021).

Beyond its industrial uses, Mn is biologically essential, acting as a cofactor for key enzymes involved in metabolism, antioxidant defense, and bone development, making it an essential metal for normal development and physiological functions (Obeng *et al.,* 2024). Normal nutritional requirements of Mn are commonly satisfied through an adequate diet, which is the normal source of the element, with minor contributions from water and air. Legumes, rice, nuts and whole grains contain the highest levels of the metal (Sobańska *et al.,* 2021). Mn is also found in seafood, seeds, chocolate, tea, leafy green vegetables, spices, soybean, and some fruits such as pineapple and acai, hence its deficiency is a rare concern. The National Research Council (NRC) recommends a dietary allowance of 2 to 5 mg/day for a safe and adequate intake of Mn for an adult human (Bayo *et al.,* 2021). However, while Mn is essential in trace amounts, excessive exposure to this metal can have detrimental effects on the body, impacting multiple organ systems and posing risks across all stages of life (Obeng *et al.,* 2024). Chronic or high-level exposure may disrupt normal physiological processes, leading to toxic outcomes that affect neurological, hepatic, and cardiovascular functions, among others (Ohiagu *et al.,* 2022).

2.1.2 Toxicokinetics

Toxicokinetics encompasses the processes of absorption, distribution, metabolism, and excretion, revealing not only how Mn enters and moves through the body but also how it can accumulate to harmful levels. Occupational exposure remains one of the primary concerns regarding Mn intoxication, particularly in industries and activities where the metal is handled regularly (Obeng *et al.,* 2024). Workers involved in mining, welding, battery production, and the application of fungicides containing Mn compounds are especially at risk. However, the risk of Mn exposure is not confined solely to miners, welders, or industrial workers (Gandhi *et al.,* 2022). The metal's widespread presence in the environment means that water and food containing elevated levels of Mn can serve as significant sources of exposure for the general population. Additionally, atmospheric Mn levels may increase due to the use of certain gasoline

additives, such as methylcyclopentadienyl manganese tricarbonyl (MMT), further contributing to potential environmental contamination (Gandhi *et al.*, 2022).

Inhalation, ingestion, and dermal contact serve as the primary routes of exposure, with occupational settings representing significant sources of inhaled Mn (Markiv *et al.*, 2023). In the general population, ingestion via the gastrointestinal tract represents the predominant pathway, as dietary sources account for most Mn intake. However, absorption through the gut is relatively limited due to homeostatic regulation by transporters and intestinal barriers that restrict excessive uptake (Gurol *et al.*, 2022). In contrast, inhalation plays a particularly significant role in occupational settings, where airborne Mn particles are deposited in the lungs. Unlike ingestion, inhaled Mn can bypass first-pass hepatic metabolism and gain direct access to the bloodstream (Gandhi *et al.*, 2022). More critically, it possesses a unique capacity to enter the central nervous system (CNS) directly through the olfactory epithelium and trigeminal nerve pathways, thereby circumventing the blood–brain barrier (Gurol *et al.*, 2022). Dermal absorption is generally negligible and does not constitute a major route of entry under ordinary conditions, although minor contributions may occur with prolonged skin contact (Markiv *et al.*, 2023).

Once absorbed, Mn is transported through the bloodstream, often binding to transferrin and other carrier proteins, and is distributed preferentially to organs rich in mitochondria, particularly the liver, kidneys, pancreas and brain, where it is rapidly concentrated (Obeng *et al.*, 2024). The brain is regarded as the most vulnerable organ to Mn intoxication, as the most severe and noticeable symptoms of Mn poisoning manifest as neurological disorders. Interestingly, Mn levels in the brain are generally lower than those found in other organs such as the liver, pancreas, bone, and kidney; however, neurons appear to be especially susceptible due to their long lifespan and high energy requirements (Obeng *et al.*, 2024). Because Mn ions are paramagnetic, their accumulation in brain tissue can be detected using T1-weighted

magnetic resonance imaging (MRI) (Jensen *et al.,* 2022). Studies in industrial workers exposed to high levels of Mn, as well as in individuals with genetic mutations affecting Mn metabolism, consistently show that Mn preferentially accumulates in the globus pallidus, followed by the putamen, caudate, midbrain, cerebellum, subthalamic nucleus, and dentate nucleus, with relative sparing of the thalamus and ventral pons (Doroszkiewicz *et al.,* 2023). Similar findings are observed in animal studies, where high manganese deposition is seen in the globus pallidus, thalamus, and substantia nigra pars compacta, followed by the caudate putamen, axonal tracts, and cortex (Doroszkiewicz *et al.,* 2023).

Mn can enter the brain through three major pathways: the blood–brain barrier (BBB), the blood–cerebrospinal fluid (CSF) barrier, and the olfactory tract (Gurol *et al.,* 2022). Following oral exposure, the BBB and blood–CSF barrier play central roles in regulating Mn entry and maintaining brain homeostasis. The BBB, which is formed by endothelial cells of cerebral capillaries, separates the blood from the brain interstitial fluid, whereas the blood–CSF barrier, composed of epithelial cells of the choroid plexus, separates the blood from the cerebrospinal fluid (Cousins *et al.,* 2022). Experimental studies have demonstrated that Mn is able to cross both barriers. These barriers are essential in protecting neuronal survival and ensuring proper CNS function by tightly regulating Mn homeostasis (McCabe and Zhao, 2021). However, in infants, the immaturity of the BBB raises concern, as it may allow higher rates of Mn entry into the developing brain, thereby increasing the risk of neurotoxicity from elevated dietary intake (Martins Jr *et al.,* 2021). In addition to these systemic routes, inhaled Mn can bypass both the BBB and blood–CSF barrier by directly entering the brain through the olfactory epithelium, a mechanism that is particularly relevant in occupational or environmental exposure to airborne Mn (Obeng *et al.,* 2024).

Mn metabolism in humans is a tightly regulated process that balances the body's requirement for this essential trace element with the need to prevent toxic accumulation. Unlike many other

metals, Mn is not stored in a single large reservoir but is instead distributed in small amounts across various tissues, including the liver, pancreas, kidney, bone, and brain (Obeng *et al.*, 2024). Among these, the liver plays the central role in regulating Mn homeostasis, acting as the primary site for both metabolism and excretion (Gandhi *et al.*, 2022). The form of Mn also influences its metabolic fate; the divalent state (Mn^{2+}) is the most biologically active and is transported into cells through specific metal transporters, including the divalent metal transporter-1 (DMT1), the transferrin receptor, and ZIP family transporters (Ray and Gaudet, 2023). Within cells, Mn participates as a cofactor in several critical enzymes, most notably manganese superoxide dismutase (MnSOD) in mitochondria, which protects against oxidative stress by scavenging reactive oxygen species (ROS). It is also required for enzymes involved in amino acid, carbohydrate, and cholesterol metabolism, as well as in the synthesis of neurotransmitters and glycoproteins (Liu *et al.*, 2022).

The elimination of absorbed Mn occurs predominantly through the bile, accounting for more than 95% of excretion, which ultimately makes the feces the primary route of Mn clearance (Gurol *et al.*, 2022). Only a very small fraction is eliminated in urine, underscoring the limited contribution of the kidneys to Mn excretion. Because of this strong dependence on the hepatobiliary pathway, impaired liver function can result in elevated systemic Mn levels and increase the risk of neurological complications (Gurol *et al.*, 2022). Within the brain, Mn enters through carrier-mediated transport mechanisms but is cleared mainly by the much slower process of diffusion. Consequently, Mn elimination from neural tissue is significantly slower than from most other organs (Chib and Singh, 2022). Its tendency to accumulate in brain regions involved in motor control, cognition, and emotional regulation creates a direct link between its toxicokinetics and the onset of clinical manifestations such as motor disturbances, memory impairment, and behaviuoral changes, which are hallmarks of Mn-induced neurotoxicity (Chib and Singh, 2022).

2.1.3 Neurotoxic Effects of Manganese

The molecular basis of Mn-induced neurotoxicity is complex and is thought to involve several interconnected pathways across different neural cell types in the brain. Evidence suggests that mitochondrial impairment, oxidative stress, neuroinflammation, and excitotoxicity play central roles in driving this toxicity (Lin *et al.,* 2022). Among these, mitochondrial dysfunction is often considered one of the earliest and most critical events, as Mn shows a tendency to accumulate within mitochondria. This accumulation disrupts normal mitochondrial function, promoting the excessive generation of ROS and reactive nitrogen species (RNS) (Jurcau, 2021). The resulting oxidative stress not only damages cellular structures but also triggers pro-inflammatory signaling cascades and activates apoptotic pathways that can lead to neuronal death (Chib and Singh, 2022).

2.1.3.1 Oxidative Stress

Oxidative stress is a key factor in a variety of pathological processes, particularly in neurodegenerative diseases such as Parkinson's disease (PD) and Alzheimer's disease (AD). Mn contributes to oxidative stress in the CNS by increasing the production of ROS, leading to oxidative damage in neural cells (Pyatha *et al.,* 2022). Experimental studies in rodents have shown that Mn-induced oxidative stress affects multiple brain regions, especially the basal ganglia, including the globus pallidus, striatum, and substantia nigra (Chib and Singh, 2022).

A major contributor to this oxidative stress is Mn-induced mitochondrial dysfunction. By inhibiting mitochondrial ATP production, Mn increases electron leakage, which in turn elevates ROS levels (Sun *et al.,* 2022). Moreover, the trivalent form of manganese (Mn^{3+}), which is an oxidized form of Mn^{2+}, is particularly potent in generating oxidative damage due to its higher oxidative stress potential. Beyond directly increasing ROS, Mn also disrupts the brain's antioxidant defense systems. It reduces the synthesis of key antioxidants such as

glutathione (GSH), depleting their levels and further amplifying the oxidative burden on neural cells (Houldsworth, 2024).

2.1.3.2 Mitochondrial Impairment and Mitophagy

Mitochondria are dynamic organelles whose primary role is the production of ATP, and their proper function is essential for neuronal health. Dysfunction of mitochondria has been strongly linked to the development of neurodegenerative diseases (Jurcau, 2021). Upon entering cells, Mn preferentially accumulates in mitochondria, making them key targets of Mn-induced neurotoxicity. Mn disrupts mitochondrial homeostasis, altering the balance of fission and fusion processes by affecting proteins such as dynamin-related protein 1 (Drp-1), optic atrophy type 1 (Opa1), and mitofusin 2 (Mfn2), which leads to mitochondrial fragmentation and impaired function (Chen *et al.,* 2023). This dysfunction contributes to oxidative stress, neuroinflammation, excitotoxicity, and ultimately apoptotic or necrotic neuronal death. The timely removal of damaged mitochondria through mitophagy, a selective form of autophagy, serves as a critical protective mechanism against Mn-induced neurotoxicity (Lu *et al.,* 2025). Mitophagy eliminates dysfunctional mitochondria, maintaining cellular health. However, prolonged exposure to Mn can impair this process, particularly by inducing S-nitrosylation of PINK1, which represses PINK1/parkin-mediated mitophagy, leading to accumulation of damaged mitochondria and neuronal injury (Lu *et al.,* 2025). Interestingly, depending on the context and duration of exposure, mitophagy can initially be activated as a protective response, but chronic Mn exposure eventually overwhelms this system, contributing to neurodegeneration (Lu *et al.,* 2025).

2.1.3.3 Inflammation

Astrocytes and microglia play essential roles in maintaining homeostasis in the CNS by regulating immune responses through the production of cytokines and other inflammatory mediators (Di Benedetto *et al.,* 2022). Research has shown that Mn disrupts mitochondrial

bioenergetics in astrocytes, triggering the release of proinflammatory cytokines that can damage neighboring neurons (Jurcau, 2022). Similarly, Mn activates microglia, which produce proinflammatory cytokines that contribute to the death of dopaminergic neurons in the rat brain. In non-human primates, Mn exposure has been shown to increase the production and release of key proinflammatory factors, including tumor necrosis factor-alpha (TNF-α), interleukin-1β (IL-1β), and inducible nitric oxide synthase (NOS2) in microglia, leading to neuronal injury (Mayer and Fischer, 2024). A central mediator of this inflammatory response is the nuclear factor kappa-light-chain-enhancer of activated B cells (NF-κB) signaling pathway, which regulates the release of microglial cytokines and amplifies the activation of astrocytes, further intensifying neuroinflammation in response to Mn toxicity (Kaur and Aran, 2025).

2.1.3.4 Autophagy

Autophagy is a vital cellular process responsible for degrading damaged organelles and macromolecules, thereby maintaining cellular homeostasis in response to stress and injury (Miller and Thorburn, 2021). Following manganese (Mn) exposure, autophagy is initially activated as a protective mechanism to limit cellular damage. However, prolonged Mn exposure impairs this process, leading to cytotoxicity and highlighting how excessive Mn disrupts normal autophagy function (Liu and Ju, 2023). Experimental studies have shown that Mn rapidly increases autophagy in the rat striatum within 4–12 hours of exposure, but at later stages—ranging from 1 to 28 days—autophagy is suppressed. Similarly, in human SH-SY5Y cells, autophagy is activated during the first 12 hours of Mn exposure but becomes impaired after 24 hours (Baj *et al.*, 2023).

This dysregulation of autophagy not only affects the turnover of cellular organelles but also activates inflammatory pathways, such as the NLRP3-CASP1 inflammasome in the hippocampus of mice and BV-2 cells, contributing to impairments in learning and memory

(Liu and Ju, 2023). In addition, Mn-induced autophagy disruption in the striatum is associated with structural changes, including an increased number of mitochondrial vacuoles, swollen and fragmented endoplasmic reticulum, and dysfunctional lysosomes, further emphasizing the detrimental effects of prolonged Mn exposure on cellular integrity (Baj *et al.*, 2023).

2.1.3.5 Glutamate excitotoxicity

Glutamate is the primary excitatory neurotransmitter in the brain, playing a central role in essential functions such as cognition, learning, and memory. However, excessive extracellular glutamate can overstimulate glutamate receptors, resulting in excitotoxic neuronal injury (Yu *et al.*, 2023). Studies have shown that manganese (Mn) disrupts glutamate homeostasis by impairing the function of astrocytic glutamate transporters, which are responsible for removing synaptic glutamate and preventing excitotoxicity (Chib and Singh, 2022). In particular, the astrocytic transporters EAAT1 (GLAST in rodents) and EAAT2 (GLT-1 in rodents) are critical for maintaining glutamate balance, and Mn exposure has been shown to reduce their expression and activity in astrocyte cultures and non-human primates (Pajarillo *et al.*, 2022). The downregulation of GLAST and GLT-1 appears to occur at the transcriptional level, mediated by increased expression of the transcription factor YY1 in the mouse brain and astrocytes. In addition to impairing glutamate uptake, Mn also enhances the sensitivity of postsynaptic glutamate receptors, further contributing to excitotoxic neuronal injury (Pajarillo *et al.*, 2022). Mn has been shown to decrease the expression of N-methyl-D-aspartate (NMDA) receptors in rats, which, alongside elevated extracellular glutamate, adds another layer to Mn's neurotoxic effects (Chib and Singh, 2022).

2.1.3.6 Apoptosis

Mn induces apoptosis through the modulation of several cellular pathways. Studies have shown that Mn triggers the activation of caspase-3, a key executor of apoptosis, as a result of endoplasmic reticulum stress (Xiang *et al.*, 2022). In the rat striatum, Mn also activates

caspase-3 and p53 signaling by increasing the neuronal expression of K-homology splicing regulator protein (KHSRP). Additionally, Mn promotes apoptosis in PC12 cells through the activation of protein kinase R and reduces the expression of wild-type p53-induced phosphatase 1, a regulator of p53 signaling in striatal neurons (Pajarillo *et al.,* 2022). Interestingly, Mn-induced apoptosis is not entirely dependent on mitochondrial impairment, as it does not always correlate with mitochondrial depolarization or the release of cytochrome C (Xiang *et al.,* 2022).

2.2 VANILLIN

Vanilla is widely regarded as one of the world's most popular and cherished flavours, obtained from the mature pods of the orchid *Vanilla planifolia* (de Oliveira *et al.,* 2022). Beyond its role as a culinary delight, vanilla has secured a strong place as a key flavouring and fragrance ingredient in ice creams, confectioneries, dairy products, perfumes, pharmaceuticals, liqueurs, and other cordial industries (Spence, 2022). This broad application has built a multimillion-dollar global market. Historically, the unique flavour of vanilla was reserved for nobility, with the Aztecs and pre-Columbian Mayas treating it as a prestigious commodity. Its introduction to the wider world came in 1519 with the Spanish conquest of the Aztecs, after which vanilla was transported to Europe (de Oliveira *et al.,* 2022). The subsequent development of hand-pollination techniques made large-scale cultivation possible and facilitated its spread to other parts of the world. At present, Madagascar stands as the leading producer of natural vanilla, contributing about 75% of global supply, followed by Indonesia, China, Mexico, and Papua New Guinea (Iftikhar *et al.,* 2023).

Chemically, vanilla is a complex mixture of around 200 compounds, but its distinctive aroma and flavour are mainly attributed to a single molecule—vanillin. Vanillin is a specialized metabolite and the principal constituent of vanilla extract, typically present at concentrations

of 1.0–2.0% (w/w) in cured vanilla beans (Sathish *et al.*, 2021). Structurally, it contains functional groups such as an aldehyde, a hydroxyl, and an ether bound to an aromatic ring, which define its characteristic physicochemical behaviour. Vanillin can be obtained either by extraction from natural vanilla beans or through chemical synthesis, most commonly from guaiacol (Arya *et al.*, 2021). In addition to its well-recognized role as a flavour and fragrance compound, vanillin has been increasingly appreciated for its diverse bioactive properties, including anticancer, neuroprotective, antibiotic-potentiating, and anti-quorum sensing activities. Therefore, due to the potential emerging reports of usage of vanillin as a therapeutic molecule and its inclusion in the food additive on generally regarded as safe (GRAS) list, it is an ideal candidate for health care applications (Arya *et al.*, 2021).

2.2.1 Sources of Vanillin

Vanillin can be obtained from three main sources: natural, synthetic (chemical), and biotechnological. The classification of vanillin as either a natural or artificial flavour largely depends on its source and the method of production (Iftikhar *et al.*, 2023). Among these, vanillin derived directly from natural vanilla or produced through biotechnological methods—such as using ferulic acid as a substrate—is widely recognized as a food-grade additive by regulatory authorities around the world (Arya *et al.*, 2021).

- ***Natural Source:*** Naturally occurring vanillin is primarily obtained from the cured pods of *Vanilla planifolia*, *Vanilla tahitensis*, and *Vanilla pompona*, which represent the major botanical sources of this compound (de Oliveira *et al.*, 2022). To isolate vanillin from these pods, several commercial extraction techniques are employed, including Soxhlet extraction, supercritical fluid extraction (SCEF), microwave- and ultrasound-assisted extraction, enzymatic extraction, solid-phase extraction, and more advanced methods such as biphasic sono electroanalysis (Arya *et al.*, 2021). Among the different types available on the market, natural vanillin remains very costly.

- ***Chemical Synthesis:*** In contrast to natural vanillin, chemically synthesized vanillin is significantly more affordable. However, it is classified as an artificial flavouring agent, which often carries negative consumer perceptions (Arya *et al.,* 2021). Over the years, a wide range of substrates have been explored for the chemical synthesis of vanillin, including lignin, guaiacol, 4-hydroxybenzaldehyde, 3-bromo-4-hydroxybenzaldehyde, 3-methoxy-4-hydroxybenzyl alcohol, cow dung, and lignin-rich agricultural residues, each with varying degrees of success (Jiang *et al.,* 2023).
- ***Biotechnological Source:*** Bioengineering represents a modern and innovative approach to vanillin production. In this method, proprietary bacterial and fungal strains are genetically engineered to convert a variety of starting materials, such as ferulic acid, eugenol, iso-eugenol, and glucose, into vanillin (Arya *et al.*, 2021). Enzymatic synthesis has also been explored, making use of proteins derived from *Nocardia* species and white-rot basidiomycetes. Looking ahead, genetically engineered plants and plant cell cultures capable of producing vanillin have been proposed as promising alternatives, offering the potential to expand both the commercial availability and the biomedical applications of vanillin (Tazon *et al.*, 2024).

2.2.2 Bioactivities

While vanillin is best known as a flavour and fragrance compound, comparatively less attention has been given to its bioactive potential. For vanillin to be considered a pharmaceutical ingredient, it must demonstrate not only relevant biological activity but also adequate bioavailability in humans and animals (Kafali *et al.,* 2024). Studies on bioavailability have examined the rate and extent of vanillin absorption into the bloodstream, plasma, and ultimately its delivery to target sites (Arya *et al.,* 2021). Toxicological evaluations further support its safety profile: vanillin has an LD_{50} of 4333 mg/kg in mice and 4730 mg/kg in rats (Salau and Islam, 2024). In addition, studies involving oral and intraperitoneal administration in rats have

shown that doses as high as 300 mg/kg are well tolerated, with no adverse effects on the liver, kidneys, or blood cells (Arya *et al.,* 2021). Interestingly, vanillin has also been reported to exhibit both hematoprotective and neuroprotective effects (Kafali *et al.,* 2024). Taken together, its non-toxic nature and promising bioactivities position vanillin as a valuable candidate for further exploration as a pharmacologically relevant bioactive molecule.

2.2.2.1 Anticancer Activity

Evidence suggesting that vanillin can influence DNA damage responses and act as an antimutagen has encouraged researchers to investigate its potential anticancer properties at both the cellular and molecular levels (Rakoczy *et al.,* 2021). Experimental studies have demonstrated that vanillin, at a concentration of 1000 µg/mL, was able to inhibit the growth of HT-29 colon cancer cells. This inhibition was marked by cell cycle arrest at the G0/G1 phase and a corresponding increase in apoptotic cells in the sub-G0 phase (Ramadoss and Sivalingam, 2020). Beyond its parent compound, derivatives of vanillin have also shown promising anticancer activity. For instance, IPM711, a vanillin-based derivative, significantly reduced the growth, invasion, and migration of HT-29 and HCT116 cells through its binding to the Wnt/β-catenin signaling receptor (Kafali *et al.,* 2024). Mechanistic insights from these studies reveal that vanillin can downregulate proteasome-related genes in colon tissue, leading to suppressed proteasome activity (Ferreira *et al.,* 2025). At higher concentrations (10 mM), it also interfered with the phosphorylation of mitogen-activated protein kinase (MAPK), thereby reducing the proliferation of granulocytes and other dividing cells, as well as lowering the number of p65-positive cells (Kafali *et al.,* 2024). Collectively, these findings suggest that the anticancer effects of vanillin may be mediated through the downregulation of proteasome genes, MAPK signaling, and nuclear factor-κB (Ferreira *et al.,* 2025).

In addition to its anticancer potential, vanillin derivatives have shown protective roles against radiation-induced damage (Rakoczy *et al.,* 2021). For example, VND3207 exhibited strong

radio-protective effects in mice with radiation-induced intestinal injury and was also found to mitigate radiation damage in human lymphoblastoid cells by enhancing the expression of DNA-PKcs, a catalytic subunit critical for the repair of DNA double-strand breaks (Li *et al*., 2020). Other in vitro studies further extend the role of vanillin in cancer therapeutics. Vanillin has been shown to trigger apoptosis in human hepatic carcinoma and neuroblastoma cells (Salau and Islam, 2024), while molecular docking studies suggest its potential binding affinity for CAMKIV, an enzyme linked to cancer progression and neurodegenerative diseases. Interestingly, vanillin dimers have also been reported to suppress the metastatic potential of HepG2 liver cancer cells by blocking the FAK/PI3K/Akt signaling pathway (Arya *et al.*, 2021). Taken together, these findings highlight vanillin and its derivatives as promising candidates for anticancer therapy.

2.2.2.2 Antioxidant and Anti-inflammatory Activity

Vanillin has attracted considerable attention for its antioxidant potential, particularly its ability to act as a potent scavenger of ROS (Kafali *et al.,* 2024). This property has been demonstrated through several well-established antioxidant assays, including the oxygen radical absorbance capacity (ORAC) assay, the $ABTS^{+}$ assay [2,2′-azino-bis (3-ethylbenzothiazoline-6-sulfonic acid)], and oxidative haemolysis inhibition tests (Arya *et al.,* 2021). Studies suggest that vanillin is highly effective in neutralizing free radicals, largely due to its unique chemical behavior (Kafali *et al.,* 2024). One important mechanism is its tendency to undergo self-dimerization, a process that allows it to react with ROS at a high stoichiometric ratio, thereby amplifying its overall antioxidant activity. Such activity is important in a biological context, since excessive ROS production has been linked to oxidative stress, cellular injury, and the pathogenesis of several chronic diseases including cancer, neurodegeneration, and cardiovascular disorders (Jomova *et al.,* 2023).

Beyond its antioxidant capacity, vanillin also exhibits significant anti-inflammatory activity. In cellular models, such as lipopolysaccharide-activated (LPS) RAW264.7 macrophages, vanillin has been shown to inhibit the overproduction of nitric oxide (NO), a pro-inflammatory mediator commonly associated with inflammatory responses (Sumayya and Muraleedhara Kurup, 2021). The suppression of nitric oxide is particularly meaningful because elevated levels are often linked to tissue damage and chronic inflammation. Mechanistic studies have revealed that this effect is closely tied to the regulation of inducible nitric oxide synthase (iNOS), the enzyme primarily responsible for NO production during inflammatory processes (Serreli and Deiana, 2023). Reverse transcription polymerase chain reaction (RT-PCR) experiments have further demonstrated that vanillin reduces the induction of iNOS messenger RNA in a concentration-dependent manner, confirming its role as a transcriptional regulator of inflammation (Kafali *et al.,* 2024).

Taken together, these findings point to a dual role of vanillin in maintaining cellular health—both as an antioxidant and as an anti-inflammatory agent. Its ability to scavenge ROS not only protects cells from oxidative damage but also complements its anti-inflammatory activity by dampening the signaling pathways that trigger chronic inflammation. These dual functions make vanillin an attractive candidate for further exploration as a natural therapeutic compound, especially in the prevention and management of oxidative stress-related and inflammatory diseases.

2.2.2.3 Neuroprotective Activity

Experimental studies in animal models provide compelling evidence that vanillin possesses strong neuroprotective properties in a range of neurological conditions, including Huntington's disease (HD) and cerebral ischemia (Salau and Islam, 2024; Arya *et al.,* 2021). In rat models of HD induced by 3-nitropropionic acid (3-NPA), vanillin treatment was found to alleviate several disease-related impairments. These included improvements in motor coordination,

locomotor activity, and learning-memory functions, along with a reduction in biochemical disturbances associated with the disease pathology (Salau and Islam, 2024). Such findings highlight vanillin's ability to act not only at the behavioral level but also at the biochemical and cellular levels, offering a multi-faceted neuroprotective response.

Further evidence supports vanillin's role in protecting specific brain regions vulnerable to ischemic injury. At a dose of 40 mg/kg, vanillin was shown to protect neurons in the hippocampal CA1 region against ischemia-induced damage (Morin *et al.,* 2021). This finding is particularly important, as the hippocampus is central to learning and memory, and its injury is strongly associated with cognitive decline following ischemic episodes (Rost *et al.,* 2022). In neonatal rat models subjected to hypoxic-ischemic brain injury, vanillin treatment promoted early neurofunctional development, reduced histomorphological damage, and significantly lowered brain infarct volume and edema (Arya *et al.,* 2021). These protective effects suggest that vanillin may play a role in preserving brain structure and function during critical developmental stages, where hypoxic-ischemic events are often devastating.

Vanillin's neuroprotective influence has also been demonstrated in models of spinal cord injury. In such cases, vanillin administration was found to reduce apoptosis in spinal tissues and downregulate the expression of hypoxia-inducible factor-α (HIF-α), a key regulator of cellular responses to low oxygen that is often upregulated in injury and stress conditions (Basheer *et al.,* 2021). The proposed mechanisms underlying these protective effects include scavenging of ROS, reduction of mitochondrial dysfunction, suppression of lipid peroxidation, and inhibition of apoptosis, all of which are critical contributors to neuronal injury and degeneration (Chen *et al.,* 2022).

More recent work has further strengthened this view by showing that vanillin and its naturally occurring analogue, vanillic acid, can modulate antioxidant defense systems (Kafali *et al.,* 2024). In studies examining Fe^{2+}-induced brain tissue damage, these compounds alleviated

metabolic complications by restoring antioxidant balance and reducing oxidative burden (Mazur *et al.*, 2024). This suggests that vanillin not only combats immediate oxidative stress but may also play a broader role in stabilizing metabolic processes that support long-term neuronal health.

2.2.2.4 Antifungal Activity

Fungal pathogens represent a major concern across multiple domains, including agriculture, food safety, and human health (Xu, 2022). They are responsible for significant crop losses, food spoilage, and in some cases, life-threatening infections in humans. With the increasing resistance of fungi to conventional antifungal agents, there is a growing interest in identifying natural compounds that can serve as safer and more sustainable alternatives. Among such candidates, vanillin has emerged as a compound of particular interest due to its demonstrated antifungal activity (Arya *et al.*, 2021).

Experimental studies have revealed that vanillin is capable of impairing the growth of a variety of fungal pathogens. For example, vanillin at a concentration of 250 mg/L was found to suppress the growth of *Alternaria* strains, fungi that are notorious for causing plant diseases and contaminating food products with harmful mycotoxins (Yang *et al.*, 2021). Vanillin exhibited fungistatic activity by extending the lag phase of the fungal life cycle from approximately 50 hours to 112 hours, thereby delaying fungal proliferation. In addition, it inhibited mycelial growth by up to 37.5%, demonstrating a direct effect on fungal structural development (Roy *et al.*, 2024). Such findings indicate that vanillin does not necessarily kill the fungus outright but slows its growth and reproduction, which can be advantageous in food preservation and crop protection (Li and Zhu, 2021).

The antifungal potential of vanillin extends beyond plant pathogens to medically important fungi. A comprehensive study evaluated vanillin and 33 of its derivatives against *Cryptococcus neoformans*, a pathogenic yeast responsible for cryptococcal meningitis, a severe opportunistic

infection especially in immunocompromised individuals. Results showed that certain derivatives, particularly o-vanillin and o-ethyl vanillin, exerted strong inhibitory effects. Transcriptomic analyses using RNA-seq revealed that these compounds disrupted mitochondrial function and induced oxidative stress within fungal cells, ultimately limiting their ability to grow and survive (Arya *et al.,* 2021). These mechanistic insights highlight that vanillin does not act as a simple fungistatic compound alone but may also target fundamental metabolic and bioenergetic pathways in pathogenic fungi (Kamel *et al.,* 2021).

The dual ability of vanillin to affect both agricultural and clinical fungal pathogens makes it a highly versatile antifungal candidate. Beyond its direct antifungal action, the relatively low toxicity and natural origin of vanillin further support its potential application in diverse industries. In the food sector, vanillin could be explored as a natural preservative to extend shelf life by controlling fungal contamination (Yang *et al.,* 2021). In agriculture, its fungistatic properties may help in reducing reliance on synthetic fungicides, thereby promoting more sustainable farming practices. Furthermore, in the pharmaceutical field, vanillin and its derivatives could be developed as adjunct or alternative therapies to treat fungal infections, particularly those resistant to current antifungal drugs (Kafali *et al.,* 2024).

Future research using advanced omics technologies, including transcriptomics, proteomics, and metabolomics, will be valuable in identifying the precise molecular targets of vanillin in fungal cells. Such approaches may not only unravel the detailed mechanisms of its antifungal action but also guide the rational design of vanillin-based derivatives with enhanced efficacy. Collectively, these insights position vanillin as a promising natural antifungal molecule with broad applications in food safety, agriculture, and medicine.

2.2.2.5 Antibacterial Activity

Vanillin has also been reported to exert antibacterial effects, particularly against spoilage and pathogenic bacteria that pose threats to food quality and human health. Studies have

demonstrated that vanillin is capable of inhibiting the growth of several bacterial species, including *Pantoea agglomerans*, *Aeromonas enteropelogenes*, *Micrococcus lylae*, and *Sphingobacterium spiritovorun* (Roy *et al.,* 2024). The minimum inhibitory concentration (MIC) values for these bacteria were found to range between 10 and 13.3 mM, suggesting that vanillin possesses a reasonably broad spectrum of antibacterial activity (Maisch *et al.,* 2022). Such findings are especially significant in the context of food preservation, as these bacteria are known contributors to spoilage and deterioration of perishable products.

Exposure of *Escherichia coli* and *Listeria innocua* to vanillin concentrations between 10–40 mM resulted in marked inhibition of cellular respiration, indicating an impairment of their energy metabolism (Wang *et al.,* 2024). At higher concentrations of 50–100 mM, vanillin treatment led to the complete dissipation of the proton ion gradient across the cell membrane in *Lactobacillus plantarum*. This disruption caused a loss of intracellular pH homeostasis, which is essential for bacterial survival and growth (Yang *et al.,* 2021). These findings suggest that vanillin's antibacterial activity may be attributed, at least in part, to its ability to interfere with bacterial membrane integrity and energy regulation.

On a molecular level, omics-based studies have further unraveled bacterial responses to vanillin. Proteomic profiling of vanillin-treated *E. coli* revealed significant changes in the abundance of approximately 147 proteins, highlighting the extensive impact of vanillin on cellular physiology (Chen *et al.,* 2023). Among the responses observed, vanillin treatment triggered an accumulation of ROS, which in turn activated adaptive stress responses mediated by transcriptional regulators such as MarA, OxyR, and SoxS. Additionally, there was an increase in RpoS/DksA-dependent gene expression, reflecting activation of global stress pathways. Interestingly, efflux systems such as AcrD and AaeAB were identified as potential mechanisms employed by bacteria to resist vanillin's effects, suggesting that bacteria may attempt to actively expel vanillin as a defense strategy (Chen *et al.,* 2023).

The growing body of evidence indicates that vanillin not only targets bacterial respiration and membrane stability but also exerts widespread effects on regulatory networks and stress responses at the molecular level. However, while these findings are promising, most studies to date have focused on food spoilage organisms or model bacteria like *E. coli* (Wang *et al.,* 2024). There remains an urgent need to extend such investigations to clinically relevant pathogens, particularly those classified as critical threats by the World Health Organization due to their rising antibiotic resistance. Advanced omics-based approaches, including transcriptomics, metabolomics, and systems biology modeling, could provide deeper insight into the gene and protein networks affected by vanillin in these pathogenic species (Sahana *et al.,* 2025).

Such knowledge would not only enhance our understanding of vanillin's antibacterial mechanisms but also open up possibilities for its application as a natural antimicrobial agent in food safety and, potentially, in therapeutic contexts. This positions vanillin as a valuable candidate in the search for novel alternatives to conventional antibiotics, particularly in the face of growing antimicrobial resistance worldwide.

2.2.2.6 Antiviral Activity

In recent years, efforts have been made to explore vanillin and its derivatives as potential antiviral agents. A particularly interesting example is the design and synthesis of a novel derivative known as MY21, which was evaluated for its anti-neuraminidase (NA) activity (Roy *et al.,* 2024). Neuraminidase is a critical viral enzyme, especially in influenza viruses, where it facilitates the release of newly formed viral particles from host cells. By inhibiting this enzyme, the viral life cycle can be disrupted, making NA an attractive target for antiviral therapy (Chauhan and Gordon, 2022).

The MY21 derivative was developed by introducing a guanidino group at the C3 position of the vanillin structure. This modification proved crucial, as it significantly enhanced NA

inhibition. Molecular modeling and docking studies further supported these findings, revealing that MY21 interacts with highly conserved and functionally essential residues within the NA active site (Arya *et al.*, 2021). The predicted binding affinities (ΔG bind values) of MY21 were found to be comparable to those of clinically used neuraminidase inhibitors such as oseltamivir and zanamivir, both of which are standard treatments for influenza infection. These results highlight the potential of vanillin derivatives as scaffolds for the development of novel antiviral drugs (Chauhan and Gordon, 2022).

Interestingly, more recent computational studies have extended this line of inquiry to coronaviruses. Early reports suggest that vanillin itself exhibits moderate binding affinity towards the spike protein and the main protease of SARS-CoV-2, the causative agent of COVID-19 (Harismah *et al.*, 2022). Since both of these viral components are essential for viral entry and replication, vanillin and its analogues could represent a promising starting point for the design of inhibitors targeting coronavirus infection. Although the binding affinities reported so far are modest, chemical modifications similar to those made in MY21 could further enhance their inhibitory potential against SARS-CoV-2 (Arya *et al.*, 2021).

Taken together, these findings indicate that vanillin and its derivatives can serve as valuable lead compounds for antiviral drug discovery. Their structural flexibility allows for modifications that can improve potency, specificity, and pharmacological properties. Moving forward, systematic structure-activity relationship (SAR) studies, combined with computational modeling, synthesis of new analogues, and experimental validation, will be essential for optimizing vanillin-based inhibitors. Such work could pave the way for the development of novel therapeutic agents not only against influenza viruses but also against emerging viral threats like SARS-CoV-2.

2.2.2.7 Antibiotic Potentiation Activity

An emerging area of interest in antimicrobial research is the ability of natural compounds such as vanillin to modulate the effectiveness of conventional antibiotics. Interestingly, studies have shown that even at sub-inhibitory concentrations, vanillin can influence bacterial susceptibility to a range of antibiotics. For example, vanillin was reported to regulate the activities of gentamicin, imipenem, norfloxacin, and spectinomycin against clinically relevant pathogens including *Pseudomonas aeruginosa*, *Staphylococcus aureus*, and *Escherichia coli* (Maisch *et al.*, 2022; Arya *et al.*, 2021). These findings indicate that vanillin, although not acting as a direct antibiotic at low concentrations, can modify bacterial responses in ways that enhance the efficacy of existing antimicrobial agents (Chen *et al.*, 2023).

More strikingly, vanillin has also been found to potentiate the activity of several commonly prescribed antibiotics, including some regarded as last-resort options for multidrug-resistant infections. In clinical isolates of extremely drug-resistant *P. aeruginosa*, vanillin enhanced the activity of chloramphenicol, ciprofloxacin, levofloxacin, tigecycline, meropenem, trimethoprim, and fosfomycin (Arya *et al.*, 2021). The ability to restore or improve the effectiveness of these antibiotics is particularly significant given the rising threat of antimicrobial resistance (AMR), which severely limits treatment options for life-threatening infections (Salam *et al.*, 2023).

The mechanisms underlying vanillin's modulatory effects are still being investigated, but they are thought to involve interference with bacterial defense systems such as efflux pumps, biofilm formation, and oxidative stress responses. By weakening these protective mechanisms, vanillin may make bacteria more vulnerable to antibiotic action. This synergistic interaction suggests that vanillin could serve as an antibiotic adjuvant—an agent used in combination with conventional antibiotics to restore or boost their activity against resistant pathogens (Kafali *et al.*, 2024).

2.3 THE CEREBELLUM

The cerebellum, whose name is derived from Latin meaning “little brain,” is a major structure of the hindbrain, weighing approximately 150 grams. It is situated in the posterior cranial fossa beneath the tentorium cerebelli, posterior to the pons and medulla oblongata (Schmahmann, 2019). Separated from the brainstem by the cavity of the fourth ventricle, the cerebellum maintains essential communication with it through three large fiber bundles known as cerebellar peduncles. The superior peduncle connects the cerebellum to the midbrain, the middle peduncle to the pons, and the inferior peduncle to the medulla oblongata (Sokolov *et al*., 2017; Murray and Antonakis, 2019). Structurally, the cerebellum exhibits remarkable organization, comprising three main parts, two surfaces, two notches, and three prominent fissures (Sokolov *et al*., 2017; Murray and Antonakis, 2019).

Grossly, the cerebellum consists of two large bilateral lobes called the cerebellar hemispheres, joined at the midline by a worm-like structure called the vermis. The vermis is divided into superior and inferior portions; the superior vermis merges seamlessly with the hemispheres, while the inferior vermis is set apart by a deep groove called the vallecula, which occupies its floor (Bostan and Strick, 2018; Schmahmann, 2019). The superior surface of the cerebellum is convex, forming a continuous surface across the hemispheres, whereas the inferior surface features the vallecular furrow, which separates the hemispheres. The anterior aspect of the cerebellum presents a wide, shallow indentation known as the anterior cerebellar notch, accommodating the pons and medulla, while posteriorly, the posterior cerebellar notch lodges the falx cerebelli.

The cerebellum is further divided by fissures into distinct lobes. The postero-lateral fissure separates the flocculonodular lobe from the larger corpus cerebelli, which is subdivided by the primary fissure into anterior and posterior lobes (Laye *et al*., 2018). The flocculonodular lobe, located on the inferior surface just anterior to the postero-lateral fissure, consists of the nodule

of the inferior vermis and paired flocculi connected to the nodule by peduncles (Bostan and Strick, 2018). The anterior lobe lies on the superior surface, anterior to the primary fissure, with its vermal portion comprising the lingula, central lobule, and culmen. The posterior lobe spans the area between the primary and postero-lateral fissures, encompassing both superior and inferior surfaces. Its superior surface contains the declive and folium, while the inferior surface includes the tuber, pyramid, and uvula (Bostan and Strick, 2018; Laye *et al*., 2018; Poeppel and Adolf, 2020).

From a phylogenetic perspective, the cerebellum can be classified into three subdivisions:

- ✓ archicerebellum
- ✓ paleocerebellum and
- ✓ neocerebellum.

The archicerebellum, or vestibular cerebellum, is the oldest part, appearing first in aquatic vertebrates such as fishes and lower amphibians. It comprises the flocculonodular lobe and lingula and is primarily connected to the vestibular system, playing a key role in maintaining equilibrium, trunk muscle tone, and posture (Murray and Antonakis, 2019; Poeppel and Adolf, 2020). The paleocerebellum, or spinal cerebellum, evolved later in terrestrial vertebrates alongside the development of limbs. It includes most of the anterior lobe, excluding the lingula, pyramid, and uvula, and through its spinocerebellar connections, it contributes to posture, muscle tone, and the coordination of crude limb movements. The neocerebellum, or cerebral cerebellum, is the most recently evolved subdivision, developing in primates alongside the expansion of the telencephalon and cerebral cortex. It primarily comprises the posterior lobe, excluding the pyramid and uvula, and is involved in cortico-ponto-cerebellar connections, facilitating the smooth execution of skilled voluntary movements. This subdivision is particularly prominent in higher mammals, reflecting its role in fine motor coordination and

complex motor control (Poeppel and Adolf, 2020; Schmahmann, 2019; Murray and Antonakis, 2019).

2.3.1 Cytoarchitecture of the Cerebellum

The cerebellum is composed of an outer layer of grey matter, known as the cerebellar cortex, and an inner layer of white matter. Embedded within the white matter are masses of grey matter called intracerebellar nuclei. The cerebellar cortex is highly folded, forming narrow, leaf-like ridges called folia. Each folium consists of a central core of white matter surrounded by a thin layer of grey matter. The white matter is arranged in a branching pattern reminiscent of a tree, which is referred to as the *arbor vitae cerebelli* (Gulani *et al*., 2017; Bostan and Strick, 2018). The grey matter of the cerebellum has two main components: the cerebellar cortex and the intracerebellar nuclei. The cerebellar cortex itself is organized into three distinct layers: the outer molecular layer, the intermediate Purkinje cell layer, and the inner granular layer (Poeppel and Adolf, 2020).

The molecular (or plexiform) layer consists of unmyelinated nerve fibers originating from the axons of granule, stellate, and basket cells, as well as the dendrites of Purkinje and Golgi cells. Stellate cells, which have short processes, are scattered near the cortical surface and form synapses with the dendrites of Purkinje cells. Basket cells, with minimal cytoplasm but extensive processes, send axons that run parallel to the cortical surface and also synapse with Purkinje cell dendrites (Bostan and Strick, 2018; Laye *et al*., 2018; King *et al*., 2019).

The Purkinje cell layer is composed of a single row of flask-shaped Purkinje cells. Their dendrites extend upward into the molecular layer, where they branch profusely and form synapses with collaterals of basket cells, axons of granule cells, and climbing fibers. The axons of Purkinje cells descend through the granular layer into the white matter, where they connect with the intracerebellar nuclei, exerting inhibitory control over these structures (Laye *et al*., 2018; Poeppel and Adolf, 2020; King *et al*., 2019).

The granular layer, the innermost layer of the cerebellar cortex, is composed of a dense population of granule cells along with a smaller number of Golgi cells. Each granule cell has dendrites that form synapses with mossy fibers, while their axons ascend into the molecular layer, bifurcating into parallel fibers that run along the long axis of the cerebellar folium and synapse with the dendrites of Purkinje cells. Golgi cells, though relatively sparse, are prominent, with dendrites that extend into the molecular layer (Laye *et al*., 2018; King *et al*., 2019; Murray and Antonakis, 2019). In the human cerebellum, there are approximately a billion granule cells, alongside millions of Purkinje, stellate, and basket cells. Collectively, the Purkinje, granule, stellate, basket, and Golgi cells constitute the intrinsic neurons of the cerebellar cortex. Notably, except for granule cells, all intrinsic neurons are inhibitory—a feature unique to the cerebellum within the central nervous system (Gulani *et al*., 2017; Caligiore *et al*., 2017; Murray and Antonakis, 2019).

The intracerebellar nuclei, also referred to as central or roof nuclei due to their proximity to the roof of the fourth ventricle, are clusters of grey matter embedded within the cerebellar white matter. Arranged from lateral to medial, these nuclei include the dentate, emboliform, globose, and fastigial nuclei (Gulani *et al*., 2017). The dentate nucleus is the largest and most prominent nucleus in primates, including humans. It belongs to the neocerebellum, receiving afferents from this region. Its shape resembles a crumpled purse, with the hilum oriented ventromedially, and its interior contains white matter composed of efferent fibers that form the majority of the superior cerebellar peduncle (Sokolov *et al*., 2017; Murray and Antonakis, 2019).

The emboliform nucleus is oval-shaped and located medial to the dentate nucleus. It belongs to the paleocerebellum, receiving input from this subdivision and sending fibers to the red nucleus via the superior cerebellar peduncle (Sokolov *et al*., 2017). The globose nucleus, situated between the emboliform and fastigial nuclei, shares similar connections with the

emboliform nucleus. Together, the emboliform and globose nuclei are referred to as the nucleus interpositus (Schmahmann, 2019).

The fastigial nucleus lies along the midline within the vermis. While smaller than the dentate nucleus, it is larger than the interposed nuclei and belongs to the archicerebellum, receiving afferents from this region and sending efferents to the vestibular and reticular nuclei (Laye *et al*., 2018). The white matter of the cerebellum is composed of three types of fibers: intrinsic, afferent, and efferent. Intrinsic fibers are confined within the cerebellum, connecting different regions either within the same hemisphere or between hemispheres. Afferent and efferent fibers link the cerebellum to other regions of the central nervous system, allowing for coordinated motor control and sensory integration (King *et al*., 2019).

2.3.2 Connections of the Cerebellum

The cerebellum maintains continuous communication with various regions of the central nervous system through an intricate network of afferent and efferent fibers. It receives input from the cerebral cortex, spinal cord, vestibular apparatus, red nucleus, and tectum of the midbrain. Cortical information reaches the cerebellum via the cortico-ponto-cerebellar, cerebro-olivo-cerebellar, and cerebro-reticulo-cerebellar pathways, while spinal input is carried by the anterior and posterior spinocerebellar tracts and the cuneocerebellar tract. Vestibular signals are conveyed either directly or via the vestibular nuclei (Bostan and Strick, 2018; Murray and Antonakis, 2019).

Afferent fibers enter the cerebellum through the middle and inferior cerebellar peduncles and are classified as climbing fibers or mossy fibers. Climbing fibers, originating from the inferior olivary nucleus, provide direct excitatory input to individual Purkinje cells and collaterals to the intracerebellar nuclei (Adamaszek *et al*., 2022). Mossy fibers, the primary afferent fibers of the cerebellum, terminate in specialized swellings called rosettes, which synapse with the dendrites of granule cells and axons of Golgi cells. This arrangement, the cerebellar

glomerulus, is spherical and encapsulated by neuroglial cells (Poeppel and Adolf, 2020; King *et al*., 2019; Murray and Antonakis, 2019). Functionally, a single climbing fiber influences one Purkinje cell, while a single mossy fiber impacts numerous granule cells, each of which connects to thousands of Purkinje cells, thereby allowing one mossy fiber to affect a wide population of Purkinje cells. Both climbing and mossy fibers provide excitatory input to Purkinje cells (Schmahmann, 2019; Schmahmann *et al*., 2019).

The efferent system of the cerebellum conveys processed information to the red nucleus, thalamus, vestibular nuclei, and reticular formation, primarily via Purkinje cells. Most Purkinje axons synapse with intracerebellar nuclei neurons, which then project to various regions of the nervous system, while some Purkinje cells from the flocculonodular lobe and vermis project directly to the lateral vestibular nuclei. Fibers from the dentate, emboliform, and globose nuclei pass through the superior cerebellar peduncle, whereas fibers from the fastigial nucleus travel through the inferior cerebellar peduncle (Poeppel and Adolf, 2020; King *et al*., 2019).

The intrinsic circuitry of the cerebellum ensures precise regulation of these signals. Afferent climbing and mossy fibers excite cerebellar cortical neurons, with collaterals also activating the intracerebellar nuclei. Climbing fibers excite Purkinje cells directly, while mossy fibers act indirectly by activating granule cells, which in turn stimulate basket and stellate cells; these inhibitory interneurons then modulate Purkinje cell activity. Mossy fibers also excite Golgi cells, which inhibit granule cells. Purkinje cells inhibit intracerebellar nuclei, which ultimately regulate muscle activity through motor areas of the brainstem and cerebral cortex (Sokolov *et al*., 2017; Caligiore *et al*., 2017; King *et al*., 2019; Schmahmann *et al*., 2019).

The cerebellar peduncles form the structural highways for these afferent and efferent fibers. The superior cerebellar peduncle (brachium conjunctivum) ascends from the anterior cerebellar notch to the tectum of the midbrain, forming the superolateral boundary of the fourth ventricle and carrying primarily efferent fibers from the dentate nucleus (Caligiore *et al*., 2017; Roland,

2023). The middle cerebellar peduncle (brachium pontis), the largest peduncle, bridges the basilar pons to the cerebellar hemispheres and is predominantly afferent. The inferior cerebellar peduncle (restiform body) connects the dorsolateral medulla oblongata with the cerebellar hemispheres and contains afferent fibers from the spinal cord, inferior olivary nucleus, reticular formation, and vestibular nuclei (Laye *et al*., 2018; Schmahmann, 2019; Murray and Antonakis, 2019). Together, this sophisticated network of afferent and efferent pathways, intrinsic circuitry, and peduncular connections enables the cerebellum to integrate sensory and motor information, fine-tune motor activity, and maintain balance, posture, and coordinated movement.

2.3.3 Functions of the Cerebellum

The cerebellum plays a central role in maintaining equilibrium, muscle tone, and posture, as well as in coordinating skilled voluntary movements by regulating the balance of muscle tension between agonist and antagonist muscles (Caligiore *et al*., 2017). Sherrington famously described the cerebellum as the "head ganglion" of the proprioceptive system, reflecting its capacity to integrate sensory input from the vestibular, visual, and auditory systems, along with information from muscle spindles, Golgi tendon organs, and tactile and pressure receptors throughout the body and head. These sensory signals are processed within the intrinsic cerebellar circuitry and subsequently integrated into the motor system through the cerebral motor cortex, red nucleus, vestibular nuclei, and reticular formation (Adamaszek *et al*., 2022; King *et al*., 2019).

When a movement is to be executed, the cerebral cortex sends commands to the anterior horn cells of the spinal cord to initiate the action, while simultaneously relaying information about the intended movement to the cerebellum. The cerebellum also receives proprioceptive feedback from muscles and joints, conveying information about the actual movement occurring. By comparing the intended movement with the actual movement, the cerebellum

detects any discrepancies and sends corrective signals to the cerebral cortex and anterior horn cells. This feedback loop ensures that movements are performed with precise timing, force, range, direction, and rate, allowing for smooth and accurate motor control (Sokolov *et al*., 2017; Bostan and Strick, 2018; King *et al*., 2019).

2.3.4 Arterial Supply of the Cerebellum

The cerebellum receives its blood supply from three paired arteries, each dedicated to specific regions and structures. The superior cerebellar artery (SCA) arises from the basilar artery and is primarily responsible for irrigating the superior surface of the cerebellum. It provides oxygenated blood to the cerebellar cortex, underlying white matter, and deep cerebellar nuclei, ensuring the proper functioning of these critical areas involved in motor coordination and postural control (Laye *et al*., 2018).

The anterior inferior cerebellar artery (AICA) also originates from the basilar artery and supplies the anterior portion of the inferior cerebellar surface. In addition to perfusing the cerebellar cortex, the AICA contributes to the blood supply of portions of the medulla oblongata. In certain cases, it gives rise to the labyrinthine artery, which supplies the inner ear, linking cerebellar perfusion to the vestibular system and balance mechanisms (Murray and Antonakis, 2019).

The posterior inferior cerebellar artery (PICA), which branches from the vertebral artery, serves the posterior region of the inferior cerebellar surface. This artery provides blood to the cerebellar cortex, the posterior cerebellar hemisphere, and critical portions of the brainstem, particularly the lateral medulla. Through these connections, the PICA not only supports cerebellar function but also plays a vital role in the integration of sensory and motor signals between the cerebellum and brainstem (King *et al*., 2019).

Together, these three paired arteries form a robust vascular network that ensures the cerebellum receives a continuous supply of oxygen and nutrients, supporting its essential roles in balance,

muscle coordination, posture, and the fine-tuning of voluntary movements. The precise distribution of these arteries allows each cerebellar subdivision—superior, anterior-inferior, and posterior-inferior surfaces—to function efficiently and maintain seamless communication with the rest of the central nervous system.

2.3.5 Venous Drainage of the Cerebellum

The venous drainage of the cerebellum is carried out by an intricate network of cerebellar veins, which channel deoxygenated blood from the cerebellar tissue into the surrounding dural venous sinuses. The superior cerebellar veins drain the upper regions of the cerebellum, including parts of the cerebellar cortex and underlying white matter, and empty into the straight sinus, transverse sinus, and superior petrosal sinus. The inferior cerebellar veins manage the drainage of the lower cerebellar regions, directing blood into the transverse, sigmoid, and occipital sinuses (King *et al*., 2019).

This well-organized venous network is essential for maintaining proper intracranial circulation and for the removal of metabolic waste products generated during cerebellar activity. Efficient venous outflow ensures that the cerebellum receives a continuous supply of oxygenated blood via its arteries, supports the high metabolic demands of its dense neuronal populations, and contributes to the overall homeostasis of the central nervous system. Disruption of this venous drainage can affect cerebellar function, potentially leading to impaired coordination, balance, and motor control.

CHAPTER THREE

MATERIALS AND METHODS

3.1 REAGENT / CHEMICALS

All reagents and chemicals were of analytical grade. They include potassium permanganate, distilled water, Na_2HPO_4, NaH_2PO_4, H_2SO_4, hydrogen peroxide, Na_2CO_3, $NaHCO_3$, EDTA-disodium, hydrochloric acid, adrenaline, pyrogallol, trichloroacetic acid, manganese chloride, vanillin, alcohol (50%, 70%, 90%, 100%), xylene, paraffin, formal saline, chloroform.

3.2 EQUIPMENT

Surgical latex glove, weighing balance, orogastric tube, measuring cylinder, conical flask volumetric flask, plastic cages, mortar and pestle, refrigerator, oven, sample bottles, water bath, paraffin dispenser, dissecting set, glass rods, rotary microtome, binocular microscope.

3.3 EXPERIMENTAL ANIMALS

The animals for this study were bred at the Animal House, Department of Anatomy, School of Basic Medical Sciences, College of Medical Sciences, University of Benin, Benin City, Edo State, Nigeria. The Wistar rats were kept in polypropylene cages at normal room temperature. The animals were fed with Chikun Feed Grower Mash (Olam Agri Holdings Pte Ltd., Lagos State, Nigeria) and had free access to water throughout the entire study period of twenty-eight days. The animals were weighed weekly before commencement and throughout the duration of the experiment using a digital weighing scale calibrated in grams and recorded to the nearest whole number. Protocols for this experiment were in accordance with the guide for the care and use of laboratory animals (National Research Council of the National Academics, 2011). Ethical approval for the study was obtained from the Research Ethics Committee, College of Medical Sciences, University of Benin, Benin City, Nigeria, with ethical approval number: **CMS/REC/2025/819.**

3.4 RESEARCH DESIGN

Forty-eight adult Wistar rats weighing between 170g and 180g were used for this study. They were randomly assigned into six groups (A, B, C, D, E, and F) of eight rats each after acclimatization to animal house conditions for three weeks with free access to feed and water.

Group	Treatment
A	Control
B	10 mg/kg body weight of manganese chloride
C	20 mg/kg body weight of Vanillin + 10 mg/kg body weight of manganese chloride
D	40 mg/kg body weight of Vanillin + 10 mg/kg body weight of manganese chloride
E	20 mg/kg body weight of Vanillin
F	40 mg/kg body weight of Vanillin

Manganese chloride was administered via intra-peritoneal route, while Vanillin was administered orally. All administrations lasted for 28 days.

3.5 NEUROBEHAVIOURAL ASSESSMENTS

To assess the effects of treatments on neurobehavioural activities, various neurobehavioural assessment tests were carried out. These include; Open field, movement initiation, string and Step tests.

3.5.1 Open Field Test

This test was conducted according to established methods of Brown *et al* (1999) and Santiago *et al* (2010). The open field test is a widely used behavioral assay designed to assess motor function and coordination. The test assesses the rat's overall locomotor activity by measuring parameters such as distance traveled, velocity, and time spent moving as well as exploratory patterns, including entries into different zones within the open field (Seibenhener and Wooten, 2015). In a 72 by 72 cm square box with lines on the floor dividing it into 18 by 18 cm squares that permitted the determination of center and peripheral sections, each rat was placed in an

open field, briefly. Each animal was then placed in the center of the field and the following parameters were measured as earlier reported by Brown *et al* (1999) and Santiago *et al* (2010):

- ***Ambulation:*** locomotor activity or movement of within the open field arena.
- ***Immobility:*** absence or minimal movement of the rat within the open field arena.
- ***Central square entry:*** total number of times the animal enters the central square with all four paws
- ***Line Crossing:*** total number of the square crossing during the test period

3.5.2 String Test

This test was conducted according to established methods of Brown *et al*. (1999) and Santiago *et al*. (2010). This was used in assessing fine motor coordination and dexterity activities. String test was used to measure grip strength and limb impairment. The rat was allowed to hold with the forepaws a steel wire (2 mm in diameter and 60 cm in length), placed at a height of 50 cm over a cushion support (Brown *et al*., 1999; Santiago *et al*., 2010). The following parameters were measured:

- ***Latency to grip loss:*** The length of time taken for the rat to lose their grip on the string. This time was recorded with cut-off time of 180 seconds. This latency to grip loss was considered as an indirect measure of grip strength (Brown *et al*., 1999; Santiago *et al*., 2010).

3.5.3 Movement Initiation Test

This test was conducted according to established methods of Brown *et al* (1999) and Santiago *et al* (2010). This was used to evaluate the ability of the animal to initiate purposeful movements. The rat was held by its trunk with its hindlimbs and one forelimb lifted above the surface of a table so that the weight of the rat's body is supported by one forelimb alone. The

time to initiate one step was recorded for each forelimb. Initiation times for both forelimbs were averaged together to make one score.

3.5.4 Step Test

This test was conducted according to established methods of Brown *et al* (1999) and Santiago *et al* (2010). The step test was used to measure postural stability. In this test, the rats were held in the same manner as in the movement initiation test, where one forelimb bears the weight of the rat. The rat is then moved laterally across a distance of 90 cm on a table top over 5 secs. The number of adjusting steps made as the rat was moved across the table was recorded for each forelimb. The average number of steps in three trials for each forelimb was recorded.

3.6 EVALUATION OF BRAIN WEIGHT

The rats were sacrificed with ketamine anesthesia (100 mg/kg), followed by cervical dislocation, once the neurobehavioral tests were finished. Rats' brains were removed from their skulls, blotted clean of blood, and instantly weighed using an electronic balance calibrated in milligrams and recorded to the nearest two decimal places. The relative brain weight was calculated as follows:

Relative brain weight = [absolute brain weight (g) / body weight of rat (g)] x 100

3.7 CEREBELLAR OXIDATIVE STRESS PARAMETERS

The harvested and weighed brains were homogenized with acid-washed sand and PBS in a porcelain mortar and pestle after being washed twice in cold phosphate-buffered saline (PBS). Then the homogenate was centrifuged at 10,000 g for 15 minutes at 4 °C, while the supernatant was gathered to estimate the results of several biochemical experiments.

3.7.1 Estimation of Catalase (CAT) activity

This was determined by the method of Cohen *et al*. (1970). Catalase is present in nearly all animal, plant, and bacteria cells. It acts to prevent the accumulation of noxious H_2O_2 which is converted to O_2 and H_2O.

- ***Preparation of reagent:*** 0.01M $KMnO_4$ was prepared by dissolving 0.158g of $KMnO_4$ in 100 ml of distilled water. Phosphate buffer (pH 7.4); 0.426 of $NaHPO_4$ NaH_2PO_4 was weighed and dissolved in 100ml of distilled water. 6M H_2SO_4: 32.3ml of conc. H_2SO_4 was added to 66.7 ml of distilled water. 30Mm H_2O_2 solution: this was prepared by measuring 0.34 ml of 30% of H_2O_2 in 1001 ml of phosphate buffer.
- ***Procedure:*** To a known volume of supernatant, (0.5ml), 5.0ml of H_2O_2 was added. This was then mixed by inversion and allowed to stand for 30 minutes. The reaction was stopped by adding 6M H_2SO_2. The absorbance was taken at 480nm within 30-60 seconds against distilled water.
- ***Calculation:*** Activity = [OD / × min × Vt] / [M × V × L ×Y]

  Where, OD= absorbance

  L= light path =1cm

  Vt = total volume of the reaction sample

  M= molar extinction co-efficient of H2O2 (40/M/cm)

3.7.2 Estimation of Malondialdehyde (MDA) activity

Malondialdehyde was determined using the thiobarbituric acid assay (Buege and Aust, 1978). Malondialdehyde which is a product of lipid peroxidation reacts with thiobarbituric acid to give a red species.

- ***Preparation of reagent:*** Stock TCA-TCB-HCL was prepared by mixing 15g of trichloroacetic acid, 0.375g of thiobarbituric acid and 0.25N hydrochloric acid. This solution was mildly heated to assist in the dissolution of the thiobarbituric acid.

- ***Procedure:*** A volume of supernatant (1.0ml) was added to 2.0ml of TCA-TBA-HCL and mixed thoroughly. The solution was heated for 15 minutes in a boiling water bath. After cooling, the flocculent precipitate was removed by centrifuging at 1000g for 10 minutes. The absorbance was determined at 535mn against a blank. The concentration MDA was determined using the formula:

$$\text{MDA (unit/mg protein)} = [(A \times Vt \times 1000)] / [(M \times V \times l \times Y)]$$

Where, A = absorbance of sample test at 535nm

Vt= total volume of the reaction = 3ml

M = molar extinction co-efficient of product= 1.56 × 105/mcm

l = light path= 1cm

V= volume of tissue extract used = 1ml

Y = mg tissue in the volume of sample used

3.7.3 Estimation of Glutathione Peroxidase (GPx) activity

This was determined by the method of Nyman (1959). This was based on the oxidation of pyrogallol to purpurogallin by peroxidase activity, resulting in a deep brown colour disposition, read at 430nm.

- ***Preparation of reagent:*** Pyrogallol (20mM): 0.2552g of pyrogallol was dissolved in 100ml of distilled water.
- ***Procedure:*** To an aliquot of supernatant (0.2ml), 2.5ml of phosphate buffer, 2.5ml of H2O2, 1.5ml of distilled water and 2.5ml of pyrogallol were added. The reaction was allowed to stand for 30 minutes at room temperature. A deep brown color was formed which was read at 420nm.
- ***Calculation:*** Activity = $[OD/Min \times VtDf] \ / \ [E \times Vs \times Y]$

OD = Absorbance of test

Vt = Total volume of reaction of reaction mixture

Df = Dilution factor = l

E = Molar extinction coefficient (12/M/cm)

Vs= volume of sample

Y = mg of protein used

3.7.4 Estimation of Superoxide Dismutase (SOD)

This was determined according to the method of Misra and Fridovich (1972)

- ***Principle:*** Adrenaline undergoes autoxidation rapidly to adrenochrome whose concentration can be determined at 420 nm with the aid of a spectrophotometer. The auto-oxidation of adrenaline depends on the presence of superoxide anions. Superoxide dismutase inhibited the auto-oxidation of adrenaline by catalyzing the breakdown of superoxide anion. The degree of inhibition reflected the activity of SOD which was determined at 420 nm.
- ***Preparation of reagents:*** Carbonate buffer (0.05 M) pH 10.2 was prepared by dissolving 0.2014 g of Na2CO3. 0.2604 g of NaHCO3 and 0.0372 g of EDTA in 100 ml of distilled water. Hydrochloric acid (0.005 M) was prepared by adding 0.044 concentrated HCl to 99.96 ml of distilled water. Adrenaline solution (0.3 mM) was prepared by dissolving 0.01098 g of Adrenaline in 100 ml of 0.005 M HCl solution.
- ***Procedure:*** A supernatant volume of 0.2 ml was mixed with 2.5 ml of carbonate buffer and 0.3 ml of adrenaline solution, and 0.2 ml of distilled water was mixed with 2.5 m of carbonate buffer and 0.3 ml adrenaline as reference sample. These were mixed and absorbance read at 420 nm.

$$\% \text{ inhibition} = [(\text{O.D test} - \text{O.D ref}) \times 100] / \text{O.}D\ test$$

Enzyme activity was calculated thus:

$$\text{SOD activity (Unit/ mg protein)} = [\%\ inhibition] / [50 \times Y]$$

Where Y = mg of protein in the volume of sample used.

3.8 HISTOLOGY OF THE CEREBELLUM

Briefly, the excised cerebellum tissues were fixed in 10% buffered formal saline. The paraffin wax embedded method of Drury and Wallington (1980) was used to prepare the tissues. They were each dehydrated for an hour at room temperature using ethanol concentrations of 70%, 90%, absolute ethanol I, and absolute ethanol II. Two xylene changes at room temperature, lasting an hour each, was used to remove the dehydrated tissue. The tissues were then soaked in two separate batches of molten paraffin wax for one hour each at 60 degrees Celsius before being embedded in multi-block paraffin wax molds. The paraffin-blocked tissues were then cut into smaller pieces and put on a wooden chuck for rotary microtome sectioning. A rotary microtome was used to slice the tissue blocks into sections that were 5m thick. To spread the parts' folded ribbons, the sections were placed in a water bath at 40 degrees Celsius. These pieces were fixed to a fresh, spotless glass slide. To increase the adherence of the sections to the slides, these were dried at 40°C using a slide drier.

3.9 HEMATOXYLIN AND EOSIN STAINING PROCEDURES

Tissue sections were deparaffinized in two changes of xylene for two minutes in each change and passed through two changes of absolute alcohol for four minutes each. They were hydrated using a series of descending grades of alcohol until water was used. Procedures of Haematoxylin and Eosin adopted on the sections was done as described by Drury and Wallington (1980). The sections were dewaxed in two changes of xylene for two minutes in each change after which they were then rehydrated in descending grades of alcohol (absolute II, absolute I, 95%, 90%, 70% and 50% ethanol) for two minutes each. Afterwards, it was then rinsed in distilled water for three minutes and stained in hematoxylin for 15-20 minutes. The excess hematoxylin stain was removed by rinsing well in running tap water for two to three minutes (sections were examined microscopically at this stage to confirm sufficient degree of staining). It was then differentiated in acid alcohol (0.5% HCL in 70% ethanol) for two to three

minutes and rinsed well in running water for 10-15 minutes before counterstaining in 1% aqueous eosin for two to four minutes. Excess stains were washed off in running water and examined under a microscope and was then dehydrated rapidly in ascending grades of ethanol (50% through absolute ethanol), cleared in xylene and mounted in a synthetic resin medium (DPX).

3.10 PHOTOMICROGRAPHY

A binocular microscope equipped with an Omax 9.0MP USB Digital Microscope Camera (manufactured in Korea) was used to take pictures of the treated slides. The camera had a 0.5X reduction lens and a 9 megapixel (3488 x 2616 pixel) high quality color digital camera. The use of 4 and 10 objective lenses was used to produce a panoramic image of the slides.

3.11 STATISTICAL ANALYSIS

Data was analyzed using GraphPad Prism statistical package (version 9). Statistical significance ($P<0.05$) was determined by means of analysis of variance (ANOVA), followed by Tukey's multiple comparison post-hoc test. Results were presented as mean ± standard error of mean (mean ± SEM).

CHAPTER FOUR

RESULTS

4.1 Effects of Treatment on Body and Brain Weight

Figure 4.1 and 4.2 show the initial and final body weights respectively, across the experimental groups. There was no significant difference ($p > 0.05$) in the initial and final body weight across the experimental groups.

Figure 4.3 shows the weight change across the experimental groups. There was a significant decrease ($p < 0.05$) in weight change of rats treated with $MnCl_2$ compared to control. However, there was a significant increase ($p < 0.05$) in the $MnCl_2$-exposed rats pre-treated with vanillin when compared to $MnCl_2$ only.

Figure 4.4 and 4.5 show the brain weight and relative brain weight respectively across the experimental groups. There was a significant decrease ($p < 0.05$) in brain weight of rats treated with $MnCl_2$ compared to control. However, there was a significant increase ($p < 0.05$) in the $MnCl_2$-exposed rats pre-treated with vanillin when compared to $MnCl_2$ only. There was no significant difference ($p > 0.05$) in the relative brain weight across the experimental groups.

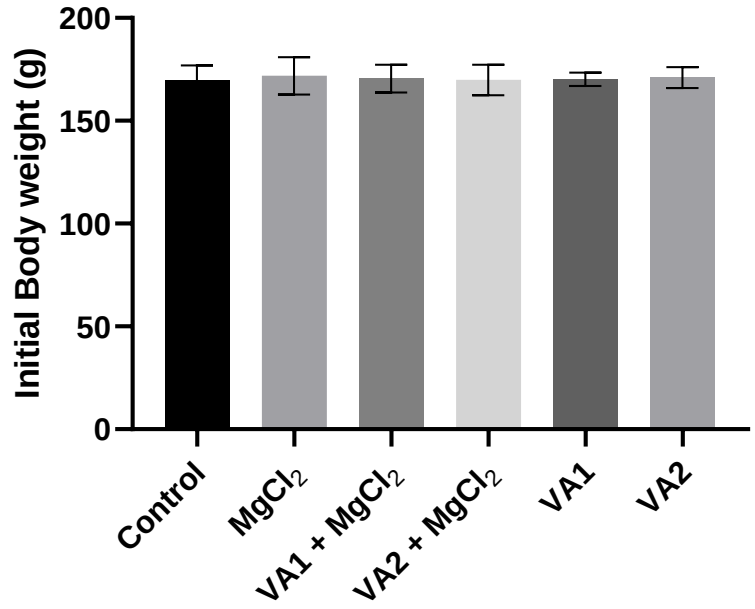

Figure 4.1: Initial body weight across experimental groups.

Values are given as mean ± SEM of each group.

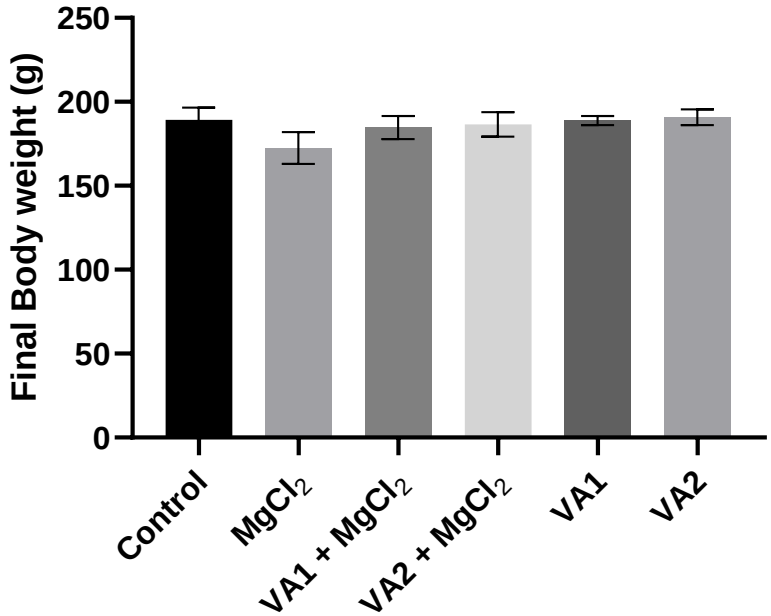

Figure 4.2: Final body weight across experimental groups.

Values are given as mean ± SEM of each group.

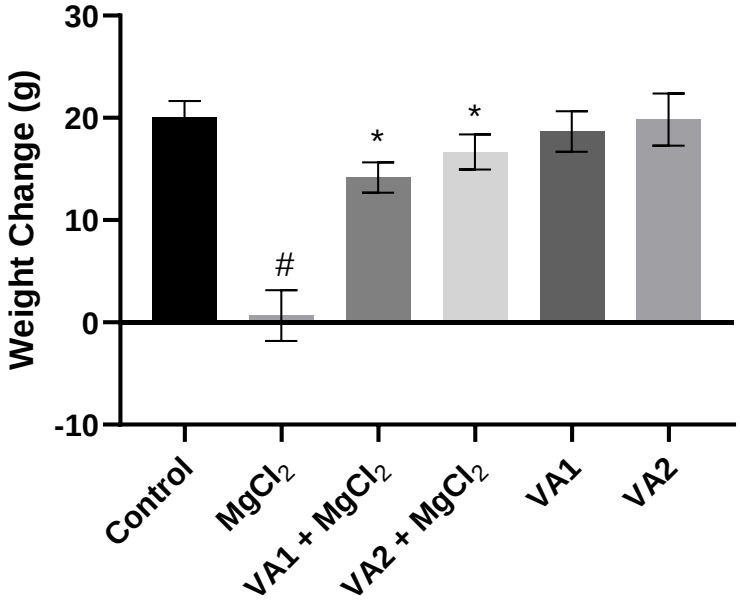

Figure 4.3: Weight change across experimental groups.

Values are given as mean ± SEM of each group. # p<0.05 compared with the control group;

* p<0.05 compared with $MnCl_2$ group

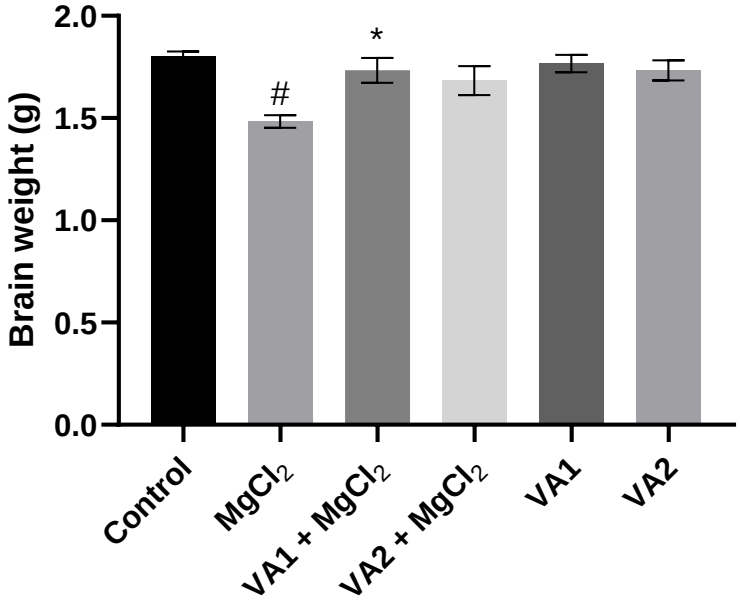

Figure 4.4: Brain weight across experimental groups.

Values are given as mean ± SEM of each group. # p<0.05 compared with the control group;

* p<0.05 compared with $MnCl_2$ group

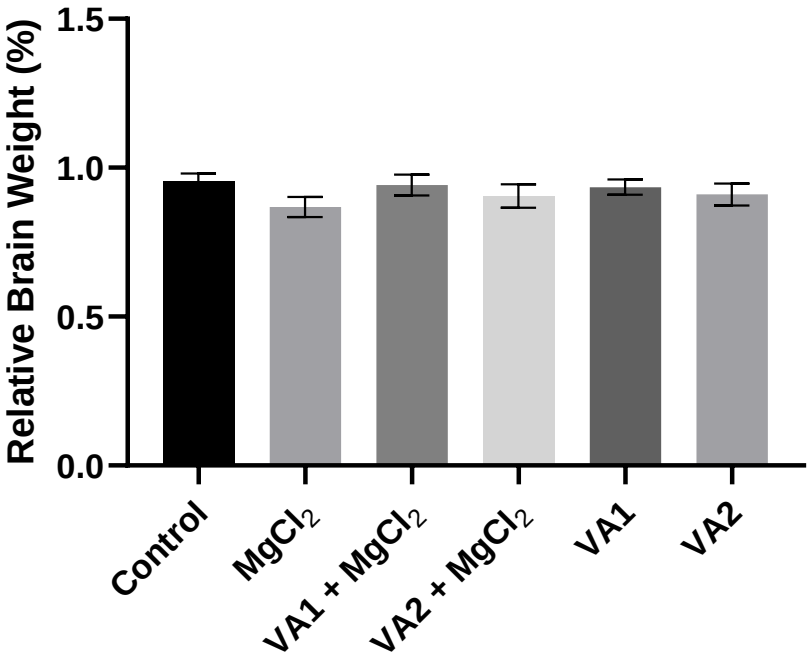

Figure 4.5: Relative brain weight across experimental groups.

Values are given as mean ± SEM of each group.

4.2 Effects of Treatment on Neurobehavioural Activity

4.2.1 Open Field Test

Figure 4.6 - 4.9 shows the ambulation, immobility, line crossing and central square entry frequency across the experimental groups. There was a significant decrease ($p < 0.05$) in the ambulation time (Fig. 4.6), line crossing frequency (Fig. 4.8) and central square (Fig. 4.9) of rats treated with $MnCl_2$ only when compared to control. However, there was a significant increase ($p < 0.05$) in the $MnCl_2$-exposed rats treated with vanillin when compared to $MnCl_2$-only. There was a significant increase ($p < 0.05$) in immobility time (Fig. 4.7) of rats treated with $MnCl_2$ only when compared to control. However, there was a significant decrease ($p < 0.05$) in the $MnCl_2$-exposed rats treated with vanillin when compared to $MnCl_2$-only.

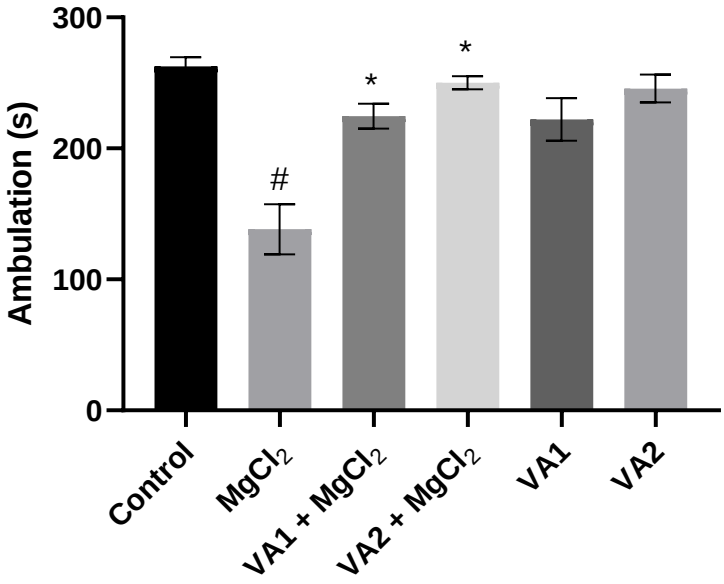

Figure 4.6: Ambulation control and treatment groups after 28 days.

Values are given as mean ± SEM of each group. # p<0.05 compared with the control group;

* *p*<0.05 compared with $MnCl_2$ group

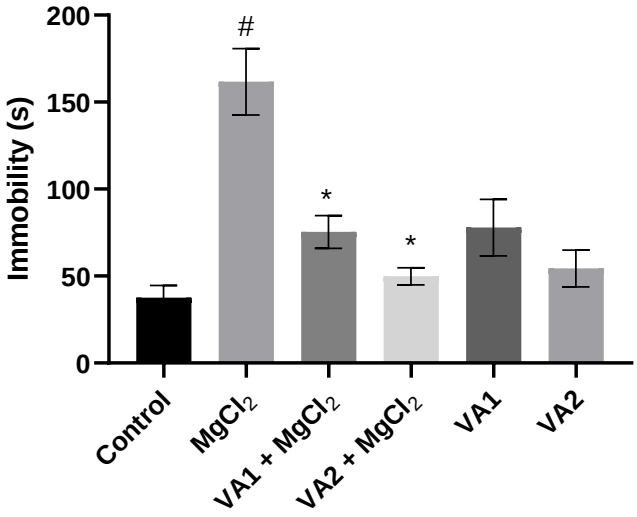

Figure 4.7: Immobility control and treatment groups after 28 days.

Values are given as mean ± SEM of each group. # p<0.05 compared with the control group;

* *p*<0.05 compared with $MnCl_2$ group.

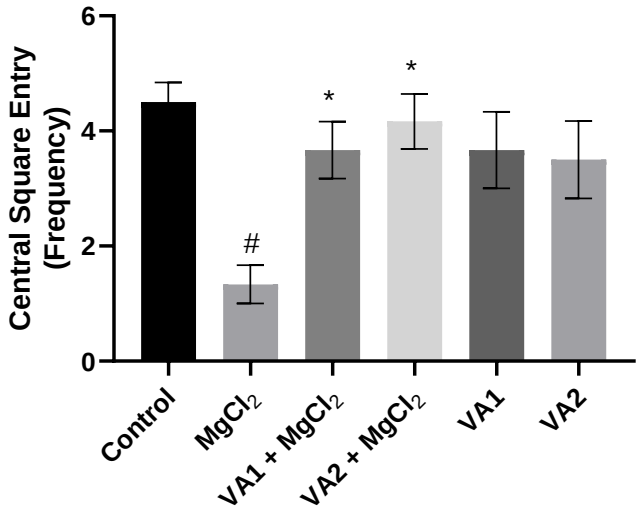

Figure 4.8: Central square entry of control and treatment groups after 28 days.

Values are given as mean ± SEM of each group. # p<0.05 compared with the control group;

* p<0.05 compared with $MnCl_2$ group.

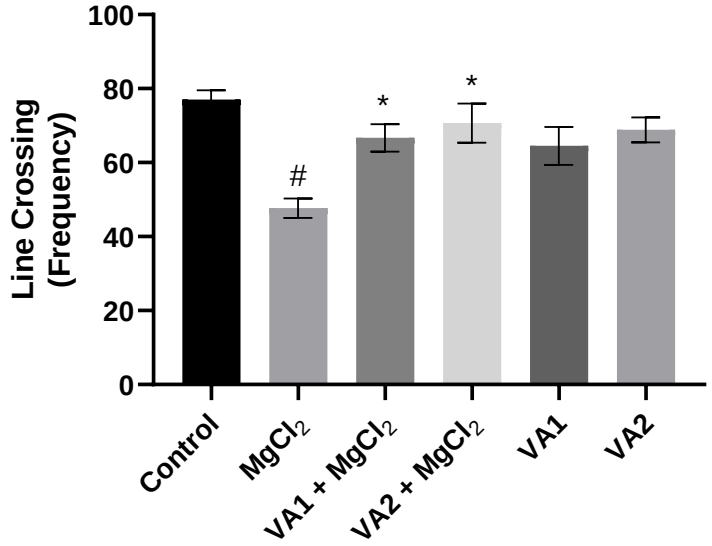

Figure 4.9: Line crossing of control and treatment groups after 28 days.

Values are given as mean ± SEM of each group. # p<0.05 compared with the control group;

* p<0.05 compared with $MnCl_2$ group.

4.2.2 String Test

Figure 4.10 shows the latency to grip loss across the experimental groups. There was a significant decrease ($p < 0.05$) in latency to grip loss of rats treated with $MnCl_2$ only when compared to control. However, there was a significant increase ($p < 0.05$) in the $MnCl_2$-exposed rats treated with vanillin when compared to $MnCl_2$-only.

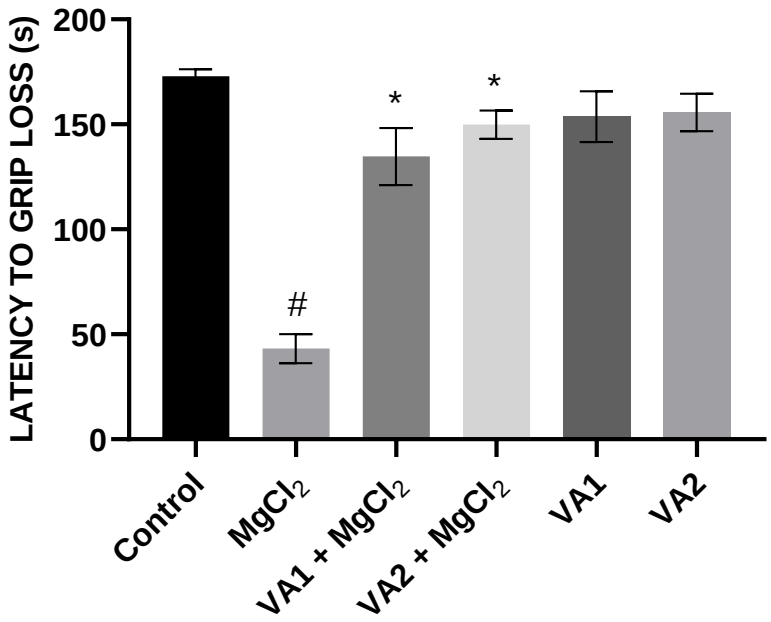

Figure 4.10: Latency to grip loss of control and treatment groups after 28 days.

Values are given as mean ± SEM of each group. # $p<0.05$ compared with the control group; * $p<0.05$ compared with $MnCl_2$ group.

4.2.3 Movement Initiation Test

Figure 4.11 shows the movement initiation across the experimental groups. There was a significant increase ($p < 0.05$) in movement initiation of rats treated with $MnCl_2$ only when compared to control. However, there was a significant decrease ($p < 0.05$) in the $MnCl_2$-exposed rats treated with vanillin when compared to $MnCl_2$-only.

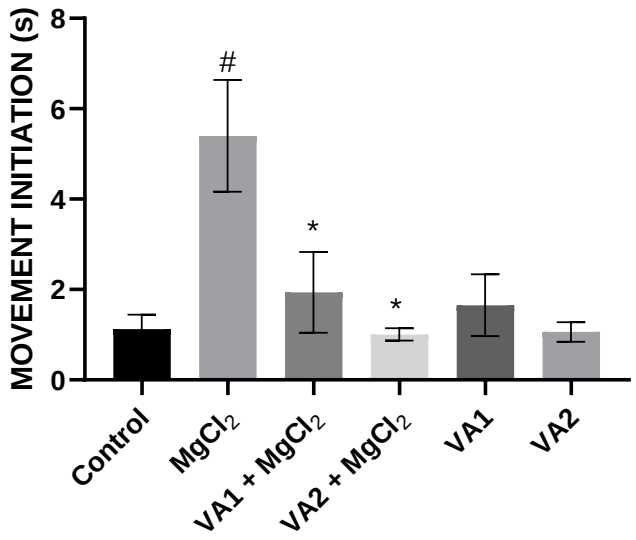

Figure 4.11: Movement Initiation of control and treatment groups after 28 days.

Values are given as mean ± SEM of each group. # $p<0.05$ compared with the control group; * $p<0.05$ compared with $MnCl_2$ group.

4.2.4 Step Test

Figure 4.12 shows the step test score across the experimental groups. There was a significant decrease ($p < 0.05$) in step test of rats treated with $MnCl_2$ only when compared to control. However, there was a significant increase ($p < 0.05$) in the $MnCl_2$-exposed rats treated with vanillin when compared to $MnCl_2$-only.

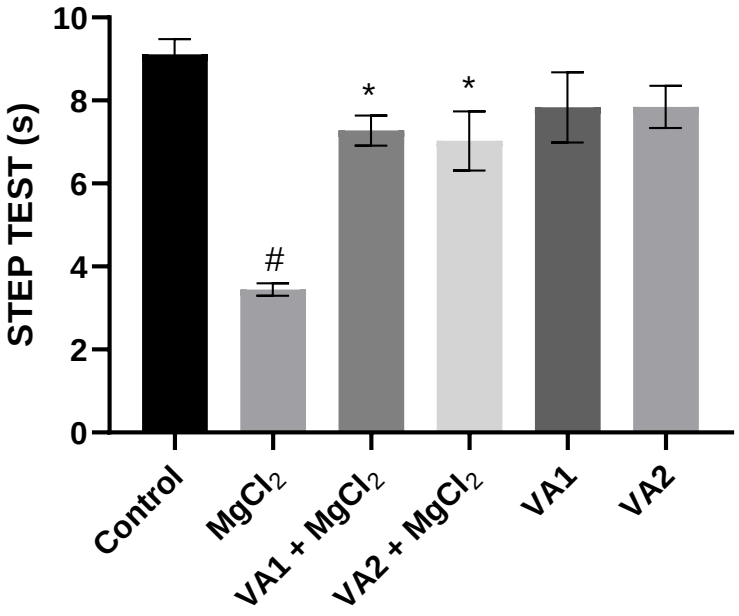

Figure 4.12: Step Test of control and treatment groups after 28 days.

Values are given as mean ± SEM of each group. # $p<0.05$ compared with the control group; * $p<0.05$ compared with $MnCl_2$ group.

4.3 Effects of Treatment on Oxidative Stress

Fig. 4.13 - 4.17 show the SOD activity, CAT activity, GPx activity, GSH concentration, and MDA levels respectively across the experimental groups. There was a significant decrease ($p < 0.05$) in SOD, CAT, GPx and GSH in the cerebellum of rats treated with $MnCl_2$-only when compared to control. However, there was a significant increase ($p < 0.05$) in the $MnCl_2$-exposed rats treated with vanillin when compared to $MnCl_2$ only. There was a significant increase ($p < 0.05$) in MDA in the cerebellum of rats treated with $MnCl_2$-only when compared to control. However, there was a significant decrease ($p < 0.05$) in the $MnCl_2$-exposed rats treated with vanillin when compared to $MnCl_2$ only.

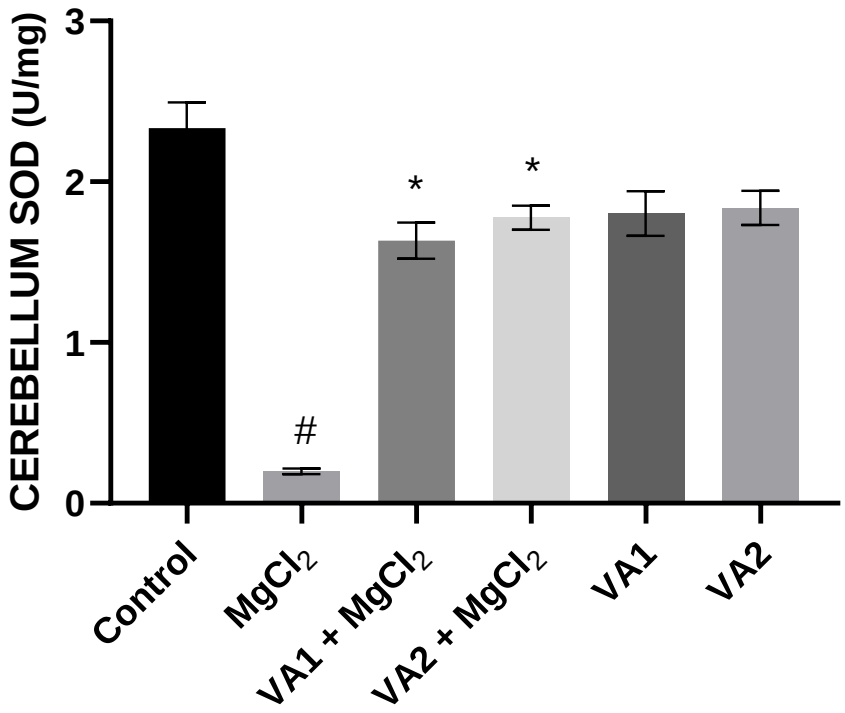

Figure 4.13: Cerebellum SOD activity of control and treatment groups after 28 days. Values are given as mean ± SEM of each group. # $p<0.05$ compared with the control group; * $p<0.05$ compared with $MnCl_2$ group.

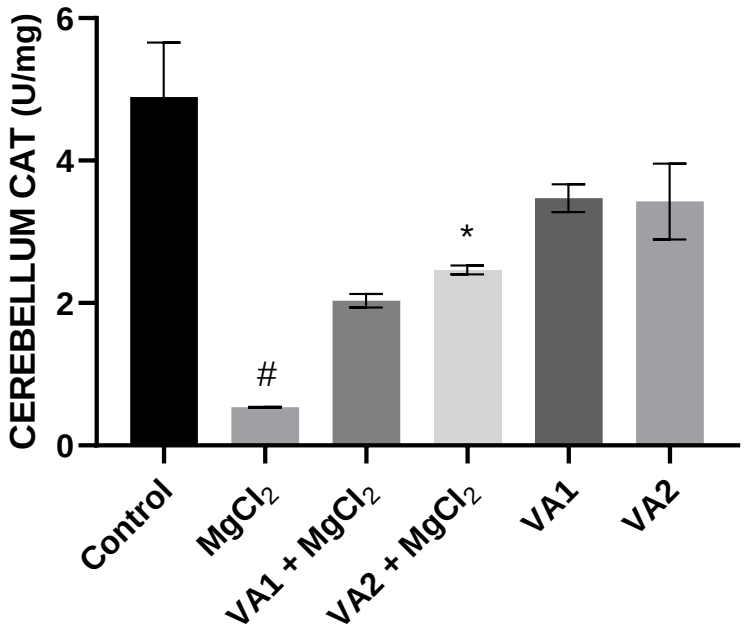

Figure 4.14: Cerebellum CAT activity of control and treatment groups after 28 days.

Values are given as mean ± SEM of each group. # p<0.05 compared with the control group;

* p<0.05 compared with $MnCl_2$ group.

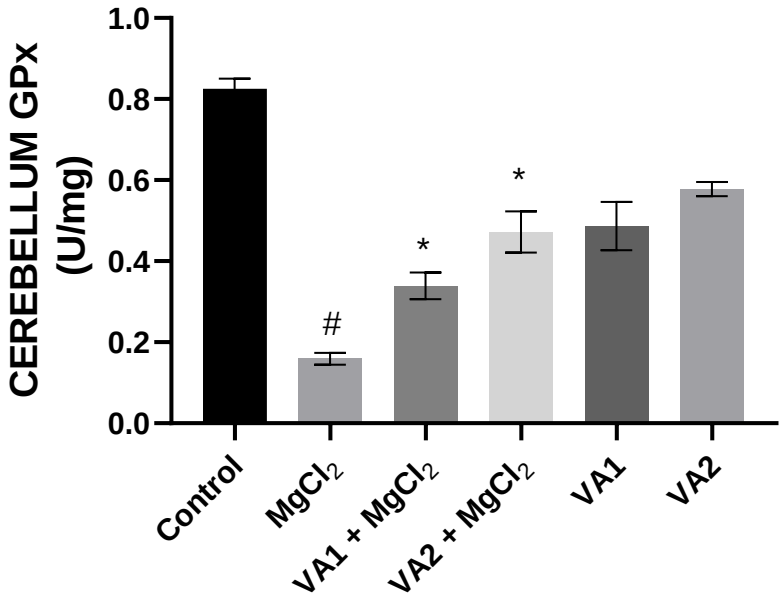

Figure 4.15: Cerebellum GPx activity of control and treatment groups after 28 days.

Values are given as mean ± SEM of each group. # p<0.05 compared with the control group;

* p<0.05 compared with $MnCl_2$ group.

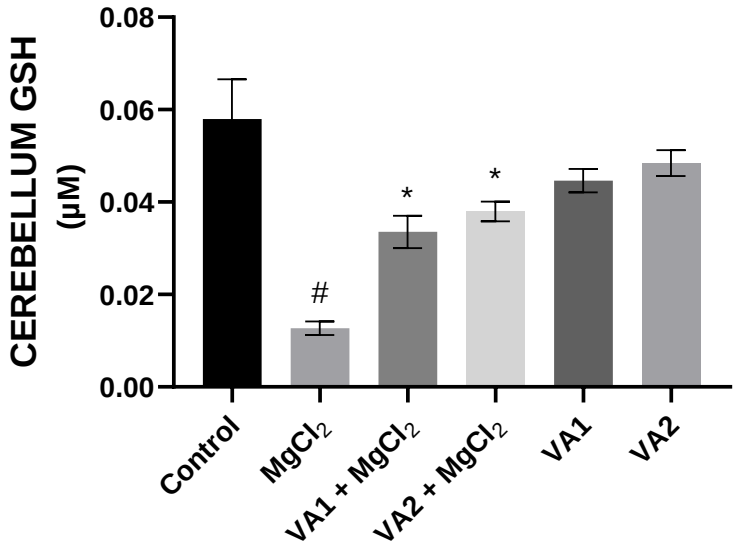

Figure 4.16: Cerebellum GSH levels of control and treatment groups after 28 days.

Values are given as mean ± SEM of each group. # p<0.05 compared with the control group;

* *p*<0.05 compared with $MnCl_2$ group.

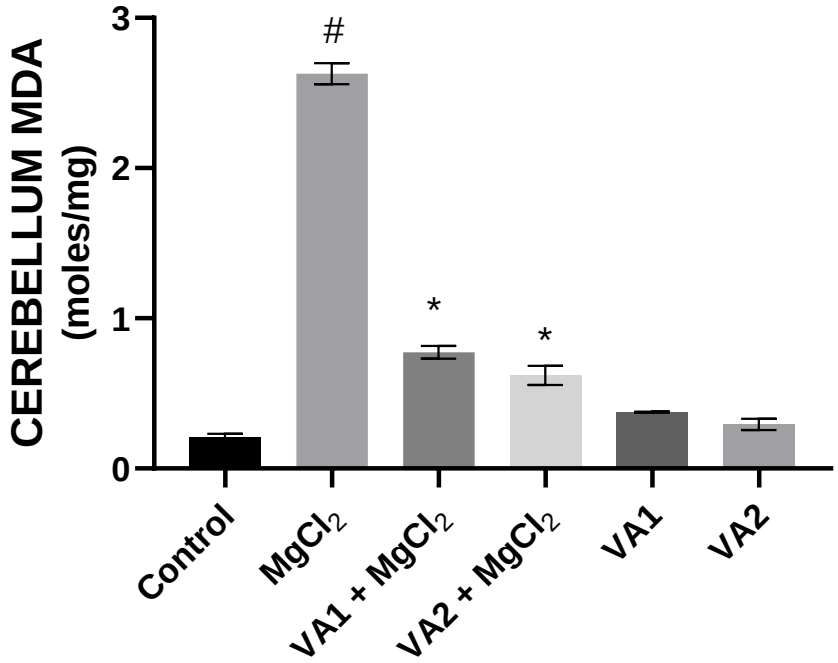

Figure 4.16: Cerebellum MDA concentration of control and treatment groups after 28 days.

Values are given as mean ± SEM of each group. # p<0.05 compared with the control group;

* *p*<0.05 compared with $MnCl_2$ group.

4.4 Effects of Treatment on Histology

Plate 4.1 - 4.6 shows the histology of the cerebellum of rats across experimental groups. Plate 4.1 shows the cerebellum histology in control group with normal histological structure with distinct molecular, Purkinje, granular layers and white mater. Plate 4.2 shows the cerebellum of rats treated with $MnCl_2$-only showing marked signs of damage, with degenerating Purkinje cells, irregular, darkly stained and pyknotic nuclei, as well as vacuolated Molecular and Purkinje cell layers. Plates 4.3 and 4.4 shows the cerebellum of $MnCl_2$-exposed rats treated with vanillin – 20 mg/kg and 40 mg/kg respectively – showing relatively normal histological structure. Plate 4.5 and Plate 4.6 shows the cerebellum of rats treated with vanillin only – 20 mg/kg and 40 mg/kg respectively showing a relatively normal histological structure.

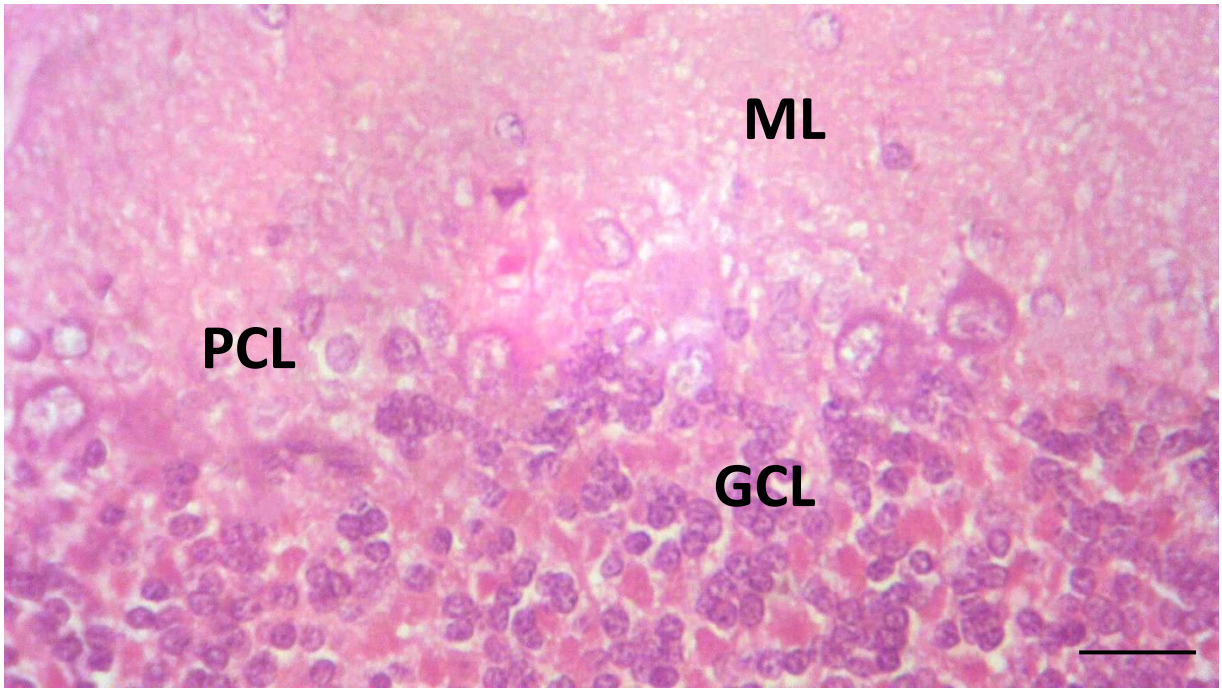

Plate 4.1: Representative histology of the cerebellum in control showing Normal histological structure of cerebellum layers – Molecular layer (ML); Purkinje Cell layer (PCL); Granular Cell layer (GCL). (HandE; Scale bar: 25µm)

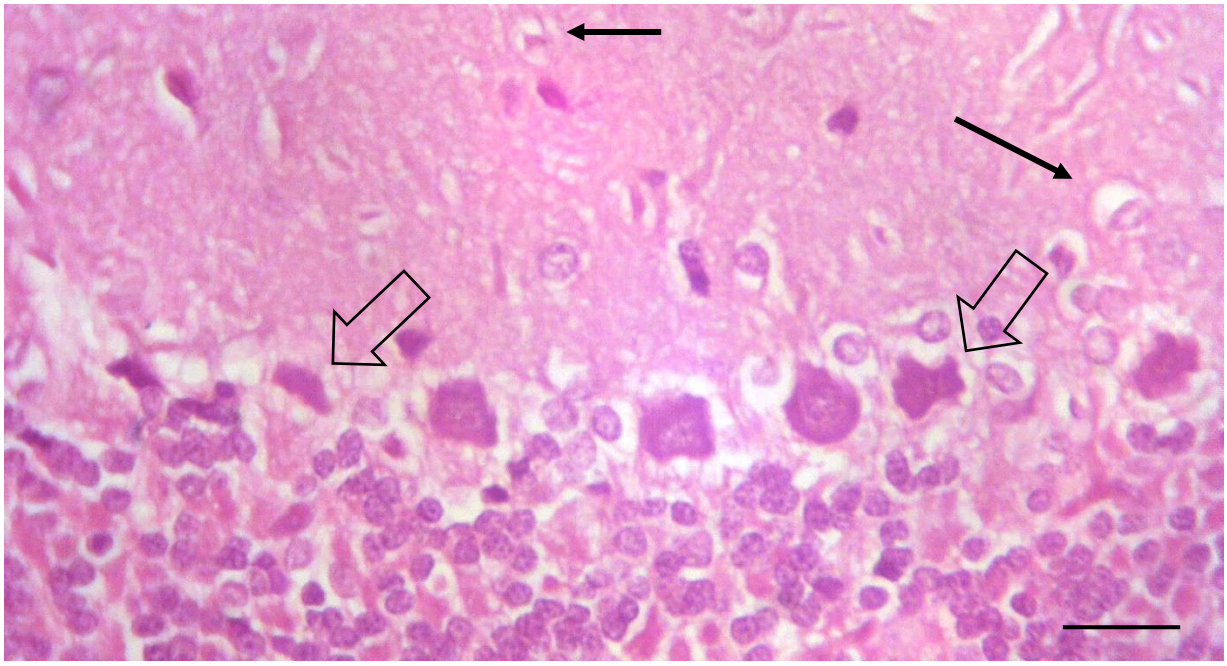

Plate 4.2: Representative histology of the cerebellum in $MnCl_2$-treated rats showing degenerating Purkinje cells (big arrows), with nuclei appearing irregular, darkly stained and pyknotic. Also observed are vacuolations in the Molecular and Purkinje cell layers (arrows). (HandE; Scale bar: 25µm)

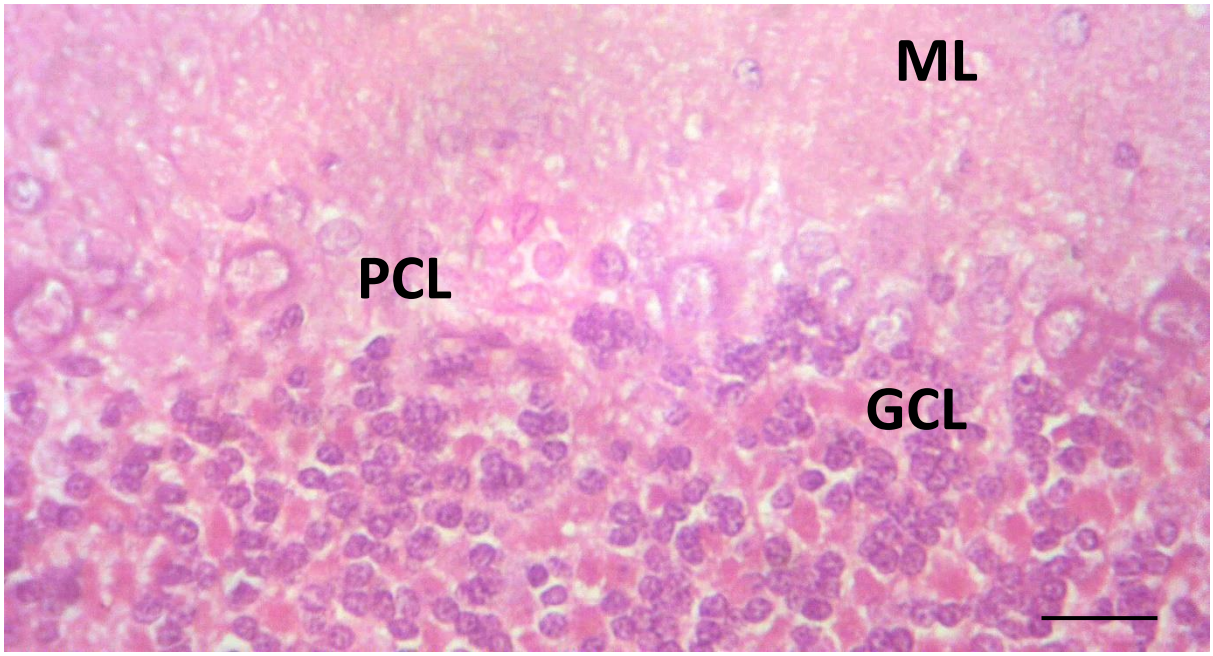

Plate 4.3: Representative histology of the cerebellum in $MnCl_2$-treated rats pre-treated with vanillin (20 mg/kg) showing showing relatively normal histological structure of cerebellum layers observed. (H&E; Scale bar: 25µm)

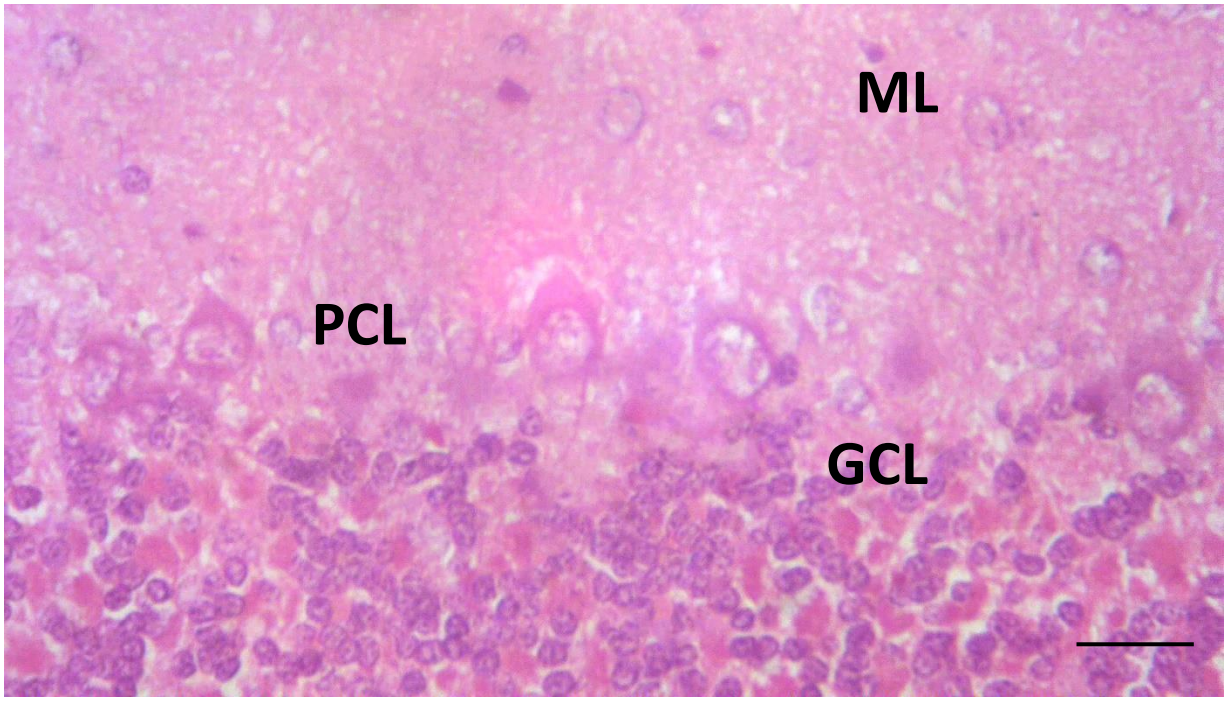

Plate 4.4: Representative histology of the cerebellum in $MnCl_2$-treated rats pre-treated with vanillin (40 mg/kg) showing showing relatively normal histological structure of cerebellum layers observed. (H&E; Scale bar: 25µm)

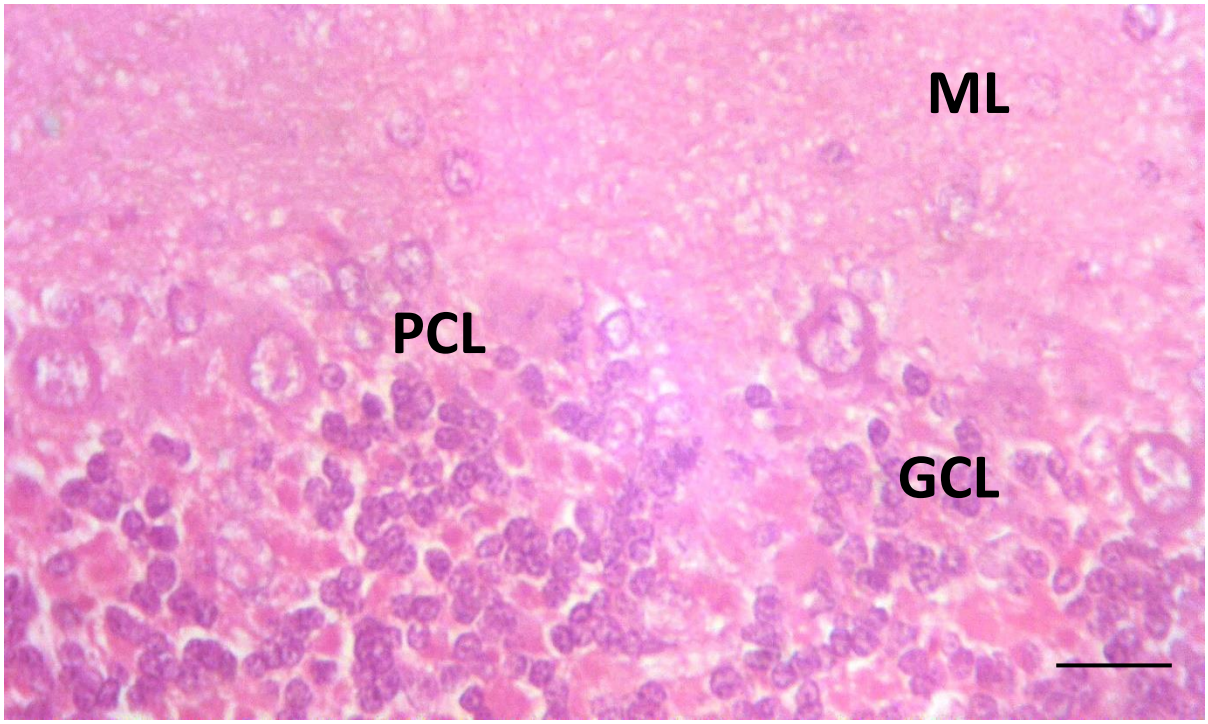

Plate 4.5: Representative histology of the cerebellum in vanillin (20 mg/kg) showing showing relatively normal histological structure of cerebellum layers observed. (H&E; Scale bar: 25µm)

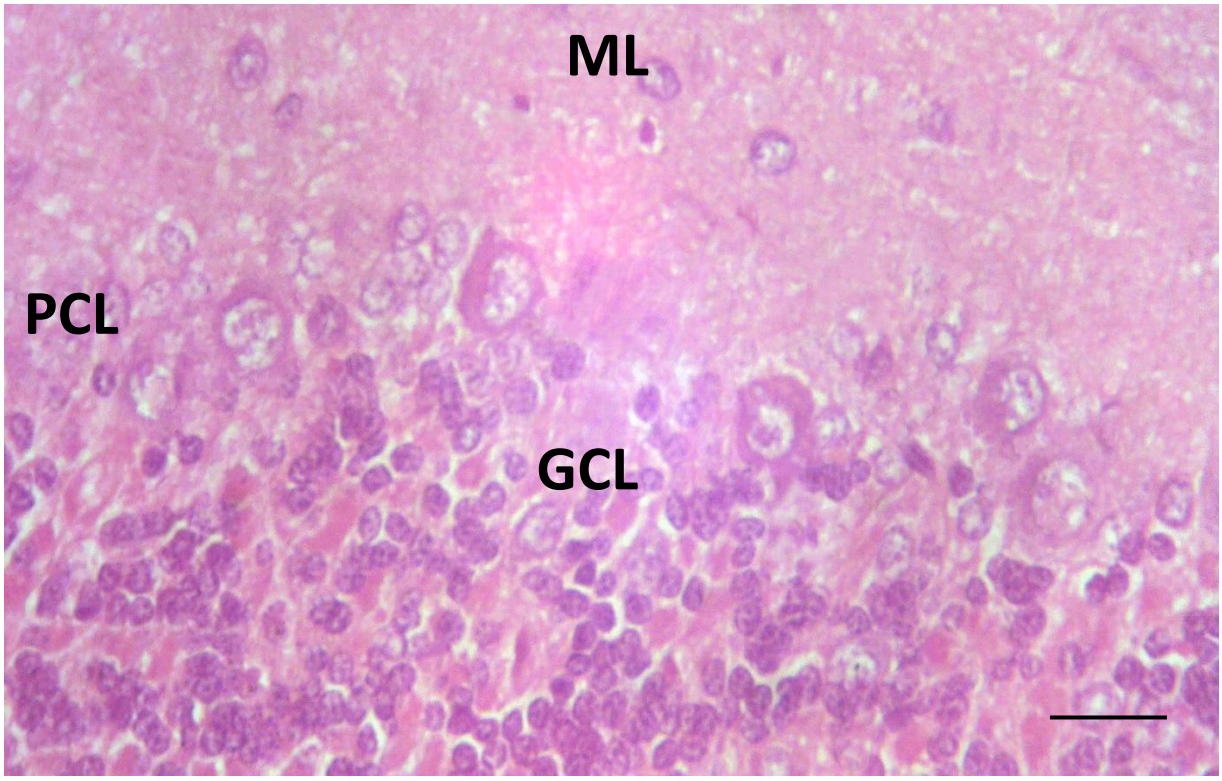

Plate 4.6: Representative histology of the cerebellum in vanillin (40 mg/kg) showing showing relatively normal histological structure of cerebellum layers observed. (H&E; Scale bar: 25µm).

CHAPTER FIVE

DISCUSSION, CONCLUSION AND RECOMMENDATION

5.1 DISCUSSION

Changes in body and organ weights are reliable indices of general health status and toxicological response in laboratory animals (Lopotych *et al*., 2020). In this study, manganese chloride ($MnCl_2$) administration produced a significant reduction in weight change, brain weight, and relative brain weight of exposed rats compared to control. These findings align with previous reports demonstrating that excessive manganese exposure disrupts normal growth and metabolic processes, leading to loss of body mass and organ atrophy (Gandhi *et al*., 2022; Jomova *et al*., 2025). Mn-induced weight reduction has been attributed to mitochondrial dysfunction and enhanced lipid peroxidation, resulting in impaired energy metabolism and protein catabolism (Jomova *et al*., 2025). Conversely, rats pre-treated with vanillin exhibited a significant increase in body and brain weights relative to $MnCl_2$-only group, suggesting that vanillin mitigated the toxic effects of Mn. The protective action of vanillin may be associated with its antioxidant and cytoprotective properties, which enhance cellular energy metabolism and reduce oxidative damage (Kafali *et al*., 2024).

The cerebellum and basal ganglia play essential roles in the regulation of coordination, posture, and voluntary movement. Disruption of these neural circuits—such as through exposure to manganese chloride ($MnCl_2$)—can produce profound motor and behavioural alterations resembling parkinsonian and cerebellar dysfunction (Jurcau, 2021; Lin *et al*., 2022). Behavioural assessments, including the open field test, string test, movement initiation, and step test, are widely employed to evaluate locomotor and coordination impairments in rodent models (Brown and Bolivar, 2018). In the Open Field Test (OFT), $MnCl_2$-treated rats displayed marked reductions in ambulation, line crossing, and central square entries, alongside increased immobility duration. These changes indicate significant locomotor inhibition, neuromuscular

impairment. Reduced ambulation and crossing frequency often reflect impaired motor coordination or basal ganglia dysfunction, while increased immobility suggests bradykinesia and reduced spontaneous activity (Enogieru and Omoruyi, 2022). The decreased central square entry further signifies increased thigmotaxis, commonly interpreted as reduced exploratory drive (Enogieru and Omoruyi, 2022). These findings are consistent with previous studies reporting that chronic Mn exposure disrupts dopaminergic and GABAergic neurotransmission in the basal ganglia and cerebellum, leading to similar behavioural outcomes (Baj *et al*., 2023; Jomova *et al*., 2025). The string test provided additional evidence of Mn-induced motor impairment. This test primarily assesses grip strength, muscular endurance, and coordination. $MnCl_2$-treated rats demonstrated reduced ability to maintain grip and poor coordination, indicating compromised neuromuscular control and cerebellar dysfunction (Enogieru and Abhelemhen, 2025). These outcomes align with observations that manganese toxicity interferes with motor pathways and synaptic signalling within cerebellar structures (Hernández *et al*., 2020; Smolyaninova *et al*., 2023). Similarly, the movement initiation test revealed significantly prolonged initiation times in $MnCl_2$-treated animals. This indicates impaired motor planning and execution, which are functions closely associated with basal ganglia and cortical motor regions. Prolonged latency in initiating movement is a hallmark of dopaminergic dysfunction and disrupted cortical–striatal communication, mechanisms known to underlie manganese-induced hypokinesia (Idemudia and Enogieru, 2025). In the step test, $MnCl_2$ exposure resulted in reduced step performance, reflecting impaired motor coordination and balance control. This decrease in stepping activity suggests compromised cerebellar regulation of movement and reduced neuromuscular precision (Idemudia and Enogieru, 2025). Collectively, results confirm that $MnCl_2$ induces widespread motor and coordination deficits consistent with cerebellar and basal ganglia dysfunction (Baj *et al*., 2023; Jomova *et al*., 2025). Remarkably, vanillin pre-treatment significantly mitigated these behavioural alterations. Rats

pre-treated with vanillin exhibited increased locomotor activity, higher line crossing and central entries, reduced immobility, and improved performance in coordination tasks compared to the $MnCl_2$-only group. These improvements may be attributed to vanillin's neuroprotective effects, mediated through the modulation of neurotransmitter balance and attenuation of oxidative stress within motor control regions (Kafali *et al*., 2024). Vanillin's antioxidant activity likely preserves dopaminergic neurons and supports mitochondrial function, thereby improving behavioural outcomes (Arya *et al.*, 2021).

Oxidative stress constitutes a fundamental mechanism underlying manganese-induced neurotoxicity (Dorman, 2023). The brain, and particularly the cerebellum, is highly vulnerable to oxidative damage due to its high oxygen consumption, abundant lipid content, and relatively modest antioxidant defense capacity (Mitoma *et al*., 2021). In the present study, exposure to $MnCl_2$ resulted in significant reductions in the activities of key antioxidant enzymes—superoxide dismutase (SOD), catalase (CAT), and glutathione peroxidase (GPx)—as well as in the levels of the non-enzymatic antioxidant glutathione (GSH). Concurrently, there was a marked elevation in malondialdehyde (MDA) concentration within cerebellar tissues, indicating increased lipid peroxidation and oxidative damage. These biochemical alterations collectively demonstrate a redox imbalance and impaired cellular defense system in $MnCl_2$-treated rats. SOD serves as the first line of defense against superoxide radicals by catalyzing their conversion to hydrogen peroxide, which is subsequently degraded by CAT and GPx (Bratovcic, 2020). Depletion of these enzymes compromises cellular antioxidant capacity, allowing hydrogen peroxide and hydroxyl radicals to accumulate, thereby damaging lipids, proteins, and DNA. The decline in GSH—a key intracellular thiol antioxidant—further exacerbates oxidative stress, as GSH participates in detoxifying reactive intermediates and maintaining redox equilibrium (Aoyama, 2021). The concomitant rise in MDA, a lipid peroxidation marker, confirms that Mn exposure disrupts membrane integrity and induces

oxidative degradation of polyunsaturated fatty acids in neural tissues (Wen and Garg, 2018; Huang *et al*., 2020). Mechanistically, Mn-induced oxidative stress has been linked to excessive generation of reactive oxygen species (ROS) and mitochondrial dysfunction. Manganese accumulates preferentially in the mitochondria, where it interferes with electron transport chain complexes, resulting in electron leakage and ROS overproduction (Bratovcic, 2020; Aoyama, 2021). The consequent oxidative burden contributes to neuronal energy failure, protein oxidation, and activation of apoptotic pathways within cerebellar neurons (Wen and Garg, 2018; Huang *et al*., 2020). These events ultimately underlie the cerebellar neurodegeneration and motor dysfunction observed in Mn toxicity. Interestingly, vanillin pretreatment markedly ameliorated these oxidative alterations. The restoration of SOD, CAT, GPx, and GSH activities, coupled with the reduction in MDA levels, indicates that vanillin exerts potent antioxidant effects capable of re-establishing redox homeostasis. This improvement may result from vanillin's ability to directly scavenge reactive oxygen species and to enhance the expression or activity of endogenous antioxidant enzymes through redox-sensitive signaling pathways (Jomova *et al*., 2023; Kafali *et al*., 2024). Moreover, vanillin's phenolic structure allows it to donate hydrogen atoms or electrons to neutralize free radicals, thereby preventing oxidative chain reactions within neural membranes (Jomova *et al*., 2023).

Histopathological findings corroborate the biochemical and behavioural data. The cerebellum of $MnCl_2$-exposed rats showed degenerating Purkinje cells, nuclear pyknosis, and vacuolation of the molecular and Purkinje cell layers, confirming structural neurodegeneration as previously described in Mn toxicity (Mohamed and Mohamed, 2017; Ali and Taha, 2019). In contrast, the cerebellar sections of $MnCl_2$-exposed rats pre-treated with vanillin displayed relatively normal cytoarchitecture, distinct cortical layers, and reduced cellular degeneration, indicating neuroprotection. This structural preservation further supports vanillin's

antioxidative and anti-apoptotic effects, likely mediated by suppression of lipid peroxidation and stabilization of neuronal membranes.

5.2 CONCLUSION

Results from this study showed that Vanillin protects against manganese chloride-induced cerebellar toxicity in Wistar rats. These findings suggest that Vanillin may serve as a potential therapeutic candidate in mitigating manganese chloride associated cerebellar dysfunction.

5.3 RECOMMENDATION

Based on the promising results of this study, further long-term *in vivo* studies are needed to confirm vanillin's efficacy and safety as a therapeutic agent for neurodegenerative diseases. Also, further investigation into the molecular mechanisms of vanillin's antioxidant and neuroprotective effects is essential. Vanillin's safety, bioavailability, and efficacy in humans, particularly for neurodegenerative conditions should be investigated.

REFERENCES

Adamaszek, M., Manto, M., & Schutter, D. J. (2022). Introduction into the Role of the Cerebellum in Emotion. In *The emotional cerebellum* (pp. 3-12). Cham: Springer International Publishing.

Ali, M. F., & Taha, M. (2019). Pathological and hematological studies on the effect of curcumin on manganese chloride-induced neurotoxicity in rats. *Comparative Clinical Pathology*, *28*(1), 69-82.

Aoyama, K. (2021). Glutathione in the Brain. *International journal of molecular sciences*, *22*(9), 5010.

Arya, S. S., Rookes, J. E., Cahill, D. M., & Lenka, S. K. (2021). Vanillin: a review on the therapeutic prospects of a popular flavouring molecule. *Advances in traditional medicine*, *21*(3), 1-17.

Baj, J., Flieger, W., Barbachowska, A., Kowalska, B., Flieger, M., Forma, A., Teresiński, G., Portincasa, P., Buszewicz, G., Radzikowska-Büchner, E., & Flieger, J. (2023). Consequences of disturbing manganese homeostasis. *International journal of molecular sciences*, *24*(19), 14959.

Banerjee, D., Das, P. K., & Mukherjee, J. (2023). Nervous System. In *Textbook of Veterinary Physiology* (pp. 265-293). Singapore: Springer Nature Singapore.

Basheer, A. S., Abas, F., Othman, I., & Naidu, R. (2021). Role of inflammatory mediators, macrophages, and neutrophils in glioma maintenance and progression: mechanistic understanding and potential therapeutic applications. *Cancers*, *13*(16), 4226.

Bayo, D., Adeniyi, O., Adeniyi, A., & Ariwoola, O. (2021). Heavy metal concentration and health risk assessment of selected fruits sold in Jos Metropolis. *Advances in Chemical Research*, *3*(2), 1-27.

Bezerra-Filho, C. S., Barboza, J. N., Souza, M. T., Sabry, P., Ismail, N. S., & de Sousa, D. P. (2019). Therapeutic potential of vanillin and its main metabolites to regulate the inflammatory response and oxidative stress. *Mini reviews in medicinal chemistry*, *19*(20), 1681-1693.

Bostan, A. C., and Strick, P. L. (2018). The basal ganglia and the cerebellum: nodes in an integrated network. Nature Reviews Neuroscience, 19(6), 338-350.

Bratovcic, A. J. A. S. (2020). Antioxidant enzymes and their role in preventing cell damage. *Acta Sci. Nutr. Health*, *4*(3), 01-07.

Brown, R. E., & Bolivar, S. (2018). The importance of behavioural bioassays in neuroscience. *Journal of Neuroscience Methods*, *300*, 68-76.

Brown, R. E., Corey, S. C. and Moore, A. K. (1999). Differences in measures of exploration and fear in MHC-congenic C57BL/6J and B6-H-2K mice. *Behavior Genetics*, 29, 263 271.

Buege J.A., and Aust S.D. 1978. Microsomal lipid peroxidation. Method in Enzymology, 52, 302-310.

Caligiore, D., Pezzulo, G., Baldassarre, G., Bostan, A. C., Strick, P. L., Doya, K., Helmich, R.C., Dirkx, M., Houk, J., Jörntell, H. and Lago-Rodriguez, A., and Herreros, I. (2017).

Consensus paper: towards a systems-level view of cerebellar function: the interplay between cerebellum, basal ganglia, and cortex. The Cerebellum, 16, 203-229.

Chauhan, R. P., & Gordon, M. L. (2022). An overview of influenza A virus genes, protein functions, and replication cycle highlighting important updates. *Virus genes*, *58*(4), 255-269.

Chen, B., Zhao, J., Zhang, R., Zhang, L., Zhang, Q., Yang, H., & An, J. (2022). Neuroprotective effects of natural compounds on neurotoxin-induced oxidative stress and cell apoptosis. *Nutritional neuroscience*, *25*(5), 1078-1099.

Chen, P., Liu, Y., Li, C., Hua, S., Sun, C., & Huang, L. (2023). Antibacterial mechanism of vanillin against Escherichia coli O157: H7. *Heliyon*, *9*(9).

Chen, W., Zhao, H., & Li, Y. (2023). Mitochondrial dynamics in health and disease: mechanisms and potential targets. *Signal transduction and targeted therapy*, *8*(1), 333.

Chib, S., & Singh, S. (2022). Manganese and related neurotoxic pathways: A potential therapeutic target in neurodegenerative diseases. *Neurotoxicology and teratology*, *94*, 107124.

Cohen, G., Dembiec, D. and Marcus, J. (1970). Measurement of catalase activity in tissue extracts. Analytical biochemistry. 34: 30 - 38.

Cousins, O., Hodges, A., Schubert, J., Veronese, M., Turkheimer, F., Miyan, J., Engelhardt, B., & Roncaroli, F. (2022). The blood–CSF–brain route of neurological disease: The indirect pathway into the brain. *Neuropathology and applied neurobiology*, *48*(4), e12789.

de Oliveira, R. T., da Silva Oliveira, J. P., & Macedo, A. F. (2022). Vanilla beyond Vanilla planifolia and Vanilla× tahitensis: Taxonomy and historical notes, reproductive biology, and metabolites. *Plants*, *11*(23), 3311.

Dey, S., Tripathy, B., Kumar, M. S., & Das, A. P. (2023). Ecotoxicological consequences of manganese mining pollutants and their biological remediation. *Environmental chemistry and ecotoxicology*, *5*, 55-61.

Di Benedetto, G., Burgaletto, C., Bellanca, C. M., Munafò, A., Bernardini, R., & Cantarella, G. (2022). Role of microglia and astrocytes in Alzheimer's disease: from neuroinflammation to Ca2+ homeostasis dysregulation. *Cells*, *11*(17), 2728.

Domingo, I., & Chieli, A. (2021). Characterizing the pigments and paints of prehistoric artists. *Archaeological and Anthropological Sciences*, *13*(11), 196.

Dorman, D. C. (2023). The role of oxidative stress in manganese neurotoxicity: a literature review focused on contributions made by Professor Michael Aschner. *Biomolecules*, *13*(8), 1176.

Doroszkiewicz, J., Farhan, J. A., Mroczko, J., Winkel, I., Perkowski, M., & Mroczko, B. (2023). Common and trace metals in Alzheimer's and Parkinson's diseases. *International journal of molecular sciences*, *24*(21), 15721.

Drury, R. A. B., and Wallington, E. A. (1980). General Staining Procedures. *In: R.A.B. Drury and E.A. Wallington (Eds.),* Carleton's Histological Techniques, 125-150. Oxford University Press, Oxford.

Engwa, G. A., Nweke, F. N., & Nkeh-Chungag, B. N. (2022). Free radicals, oxidative stress-related diseases and antioxidant supplementation. *Alternative Therapies in Health & Medicine*, *28*(1).

Enogieru, A. B., & Abhelemhen, G. I. (2025). Cerebellar alterations following mercury chloride exposure in Wistar rats: protective role of folic acid. *Scientia Africana*, *24*(2), 69-78.

Enogieru, A., & Omoruyi, S. (2022). Exploration of aqueous Phyllanthus amarus leaf extract as a protective agent in mercury chloride-exposed wistar rats: A neurobehavioural study. *Journal of Applied Sciences and Environmental Management*, *26*(4), 629-637.

Ferreira, S., Menezes, R., Trougakos, I., Gumeni, S., Bolanos-García, V., dos Santos, C. N., & Ávila-Gálvez, M. Á. (2025). Shedding Light Towards the Power of Phenolic Metabolites as Dynamic Modulators of the Ubiquitin-Proteasome System in Chronic Diseases.

Gandhi, D., Rudrashetti, A. P., & Rajasekaran, S. (2022). The impact of environmental and occupational exposures of manganese on pulmonary, hepatic, and renal functions. *Journal of Applied Toxicology*, *42*(1), 103-129.

Gulani, V., Calamante, F., Shellock, F. G., Kanal, E., and Reeder, S. B. (2017). Gadolinium deposition in the brain: summary of evidence and recommendations. The Lancet Neurology, 16(7), 564-570.

Gurol, K. C., Aschner, M., Smith, D. R., & Mukhopadhyay, S. (2022). Role of excretion in manganese homeostasis and neurotoxicity: A historical perspective. *American Journal of Physiology-Gastrointestinal and Liver Physiology*, *322*(1), G79-G92.

Harismah, K., Fazeli, F., & Zandi, H. (2022). Structural analyses of vanillin derivative compounds and their molecular docking with mpro and rdrp enzymes of covid-19. *Biointerface Res. Appl. Chem*, *12*(2), 1660-1669.

Hernández, R. B., Carrascal, M., Abian, J., Michalke, B., Farina, M., Gonzalez, Y. R., & Suñol, C. (2020). Manganese-induced neurotoxicity in cerebellar granule neurons due to perturbation of cell network pathways with potential implications for neurodegenerative disorders. *Metallomics*, *12*(11), 1656-1678.

Houldsworth, A. (2024). Role of oxidative stress in neurodegenerative disorders: a review of reactive oxygen species and prevention by antioxidants. *Brain Communications*, *6*(1), fcad356.

Huang, Z., Chen, Y., & Zhang, Y. (2020). Mitochondrial reactive oxygen species cause major oxidative mitochondrial DNA damages and repair pathways. *Journal of biosciences*, *45*(1).

Iannuzzi, C., Liccardo, M., & Sirangelo, I. (2023). Overview of the role of vanillin in neurodegenerative diseases and neuropathophysiological conditions. *International Journal of Molecular Sciences*, *24*(3), 1817.

Idemudia, O. U., & Enogieru, A. B. (2025). Upregulation of Caspase-3 and TNF-α in a rat model of cerebellar motor disorder: role of Cucumis sativus (cucumber). *Journal of Molecular Histology*, *56*(3), 191.

Iftikhar, T., Majeed, H., Waheed, M., Zahra, S. S., Niaz, M., & AL-Huqail, A. A. (2023). Vanilla. In *Essentials of medicinal and aromatic crops* (pp. 341-371). Cham: Springer International Publishing.

Ijomone, O. M., Ifenatuoha, C. W., Aluko, O. M., Ijomone, O. K., & Aschner, M. (2020). The aging brain: impact of heavy metal neurotoxicity. *Critical reviews in toxicology*, *50*(9), 801-814.

Jensen, N., Terrell, R., Ramoju, S., Shilnikova, N., Farhat, N., Karyakina, N., Cline, B.H., Momoli, F., Mattison, D., & Krewski, D. (2022). Magnetic resonance imaging T1 indices of the brain as biomarkers of inhaled manganese exposure. *Critical Reviews in Toxicology*, *52*(5), 358-370.

Jiang, W., Chen, X., Feng, Y., Sun, J., Jiang, Y., Zhang, W., Xin, F., & Jiang, M. (2023). Current status, challenges, and prospects for the biological production of vanillin. *Fermentation*, *9*(4), 389.

Jomova, K., Alomar, S. Y., Valko, R., Nepovimova, E., Kuca, K., & Valko, M. (2025). The role of redox-active iron, copper, manganese, and redox-inactive zinc in toxicity, oxidative stress, and human diseases. *EXCLI journal*, *24*, 880.

Jomova, K., Raptova, R., Alomar, S. Y., Alwasel, S. H., Nepovimova, E., Kuca, K., & Valko, M. (2023). Reactive oxygen species, toxicity, oxidative stress, and antioxidants: chronic diseases and aging. *Archives of toxicology*, *97*(10), 2499-2574.

Jurcau, A. (2021). Insights into the pathogenesis of neurodegenerative diseases: Focus on mitochondrial dysfunction and oxidative stress. *International journal of molecular sciences*, *22*(21), 11847.

Jurcău, M. C., Andronie-Cioara, F. L., Jurcău, A., Marcu, F., Ţiț, D. M., Pașcalău, N., & Nistor-Cseppentö, D. C. (2022). The link between oxidative stress, mitochondrial dysfunction and neuroinflammation in the pathophysiology of Alzheimer's disease: therapeutic implications and future perspectives. *Antioxidants*, *11*(11), 2167.

Kafali, M., Finos, M. A., & Tsoupras, A. (2024). Vanillin and its derivatives: a critical review of their anti-inflammatory, anti-infective, wound-healing, neuroprotective, and anti-cancer health-promoting benefits. *Nutraceuticals*, *4*(4), 522-561.

Kamel, E. M., Maodaa, S., Al-Shaebi, E. M., & Lamsabhi, A. M. (2024). Mechanistic insights into the metabolic pathways of vanillin: unraveling cytochrome P450 interaction mechanisms and implications for food safety. *Organic & biomolecular chemistry*, *22*(32), 6561-6574.

Katiyar, P., Ghosh, S., Saini, S., Ghosh, C., Agrawal, H., Sircar, D., & Roy, P. (2022). Antioxidant nutraceuticals as novel neuroprotective agents. *Handbook of nutraceuticals and natural products: biological, medicinal, and nutritional properties and applications*, *1*, 127-168.

Kaur, M., & Aran, K. R. (2025). Unraveling the role of Nrf2 in dopaminergic neurons: A review of oxidative stress and mitochondrial dysfunction in Parkinson's disease. *Metabolic Brain Disease*, *40*(2), 123.

King, M., Hernandez-Castillo, C. R., Poldrack, R. A., Ivry, R. B., and Diedrichsen, J. (2019). Functional boundaries in the human cerebellum revealed by a multi-domain task battery. Nature neuroscience, 22(8), 1371-1378.

Kulshreshtha, D., Ganguly, J., & Jog, M. (2021). Manganese and movement disorders: a review. *Journal of movement disorders*, *14*(2), 93.

Laye, S., Nadjar, A., Joffre, C., and Bazinet, R. P. (2018). Anti-inflammatory effects of omega 3 fatty acids in the brain: physiological mechanisms and relevance to pharmacology. Pharmacological reviews, 70(1), 12-38.

Li, M., Lang, Y., Gu, M. M., Shi, J., Chen, B. P., Yu, L., Zhou, P.K., & Shang, Z. F. (2020). Vanillin derivative VND3207 activates DNA-PKcs conferring protection against radiation-induced intestinal epithelial cells injury in vitro and in vivo. *Toxicology and applied pharmacology*, *387*, 114855.

Li, Q., & Zhu, X. (2021). Vanillin and its derivatives, potential promising antifungal agents, inhibit Aspergillus flavus spores via destroying the integrity of cell membrane rather than cell wall. *Grain & oil science and technology*, *4*(2), 54-61.

Lin, M. M., Liu, N., Qin, Z. H., & Wang, Y. (2022). Mitochondrial-derived damage-associated molecular patterns amplify neuroinflammation in neurodegenerative diseases. *Acta Pharmacologica Sinica*, *43*(10), 2439-2447.

Liu, C., & Ju, R. (2023). Manganese-induced neuronal apoptosis: new insights into the role of endoplasmic reticulum stress in regulating autophagy-related proteins. *Toxicological Sciences*, *191*(2), 193-200.

Liu, M., Sun, X., Chen, B., Dai, R., Xi, Z., & Xu, H. (2022). Insights into manganese superoxide dismutase and human diseases. *International journal of molecular sciences*, *23*(24), 15893.

Lodge, E. K. (2022). *Social and Environmental Risk Factors for Elevated Serum Metals and Their Role in Epigenetic Aging* (Doctoral dissertation, The University of North Carolina at Chapel Hill).

Lopotych, N., Panas, N., Datsko, T., & Slobodian, S. (2020). Influence of heavy metals on hematologic parameters, body weight gain and organ weight in rats. *Ukrainian Journal of Ecology*, *10*(1), 175-179.

Lu, Y., Gao, L., Yang, Y., Shi, D., Zhang, Z., Wang, X., Huang, Y., Wu, J., Meng, J., Li, H., & Yan, D. (2025). Protective role of mitophagy on microglia-mediated neuroinflammatory injury through mtDNA-STING signaling in manganese-induced parkinsonism. *Journal of Neuroinflammation*, *22*(1), 55.

Lucchini, R., Placidi, D., Cagna, G., Fedrighi, C., Oppini, M., Peli, M., & Zoni, S. (2017). Manganese and developmental neurotoxicity. *Neurotoxicity of Metals*, 13-34.

Maisch, N. A., Bereswill, S., & Heimesaat, M. M. (2022). Antibacterial effects of vanilla ingredients provide novel treatment options for infections with multidrug-resistant bacteria–A recent literature review. *European Journal of Microbiology and Immunology*.

Manessis, G., Kalogianni, A. I., Lazou, T., Moschovas, M., Bossis, I., & Gelasakis, A. I. (2020). Plant-derived natural antioxidants in meat and meat products. *Antioxidants*, *9*(12), 1215.

Markiv, B., Expósito, A., Ruiz-Azcona, L., Santibáñez, M., & Fernández-Olmo, I. (2023). Environmental exposure to manganese and health risk assessment from personal

sampling near an industrial source of airborne manganese. *Environmental Research*, *224*, 115478.

Martins Jr, A. C., Ruella Oliveira, S., Barbosa Jr, F., Tinkov, A. A., V. Skalny, A., Santamaría, A., Lee, E., Bowman, A.B., & Aschner, M. (2021). Evaluating the risk of manganese-induced neurotoxicity of parenteral nutrition: Review of the current literature. *Expert opinion on drug metabolism & toxicology*, *17*(5), 581-593.

Mayer, M. G., & Fischer, T. (2024). Microglia at the blood brain barrier in health and disease. *Frontiers in Cellular Neuroscience*, *18*, 1360195.

Mazur, T., Malik, M., & Bieńko, D. C. (2024). The impact of chelating compounds on Cu2+, Fe2+/3+, and Zn2+ ions in Alzheimer's disease treatment. *Journal of inorganic biochemistry*, *257*, 112601.

McCabe, S. M., & Zhao, N. (2021). The potential roles of blood–brain barrier and blood–cerebrospinal fluid barrier in maintaining brain manganese homeostasis. *Nutrients*, *13*(6), 1833.

Miller, D. R., & Thorburn, A. (2021). Autophagy and organelle homeostasis in cancer. *Developmental cell*, *56*(7), 906-918.

Misra, H.P. and Fridovich, I. (1972). The role of superoxide anion in the autoxidation of epinephrine and a simple assay for superoxide dismutase. *The Journal of Biological Chemistry*. 247(10), 3170 - 3175.

Mitoma, H., Manto, M., & Shaikh, A. G. (2021). Mechanisms of ethanol-induced cerebellar ataxia: underpinnings of neuronal death in the cerebellum. *International journal of environmental research and public health*, *18*(16), 8678.

Mohamed, H., & Mohamed, H. (2017). The Effect of Prenatal and Postnatal Administration of Manganese Chloride on the Developing Caudate Nucleus of the Corpus Striatum in Male Albino Rats and the Possible Beneficial Role of Vitamin E Supplementation: A Histological and Immunohistochemical study. *The Egyptian Journal of Anatomy*, *40*(2), 203-236.

Morin, A., Poitras, M., & Plamondon, H. (2021). Global cerebral ischemia in adolescent male Long Evans rats: Effects of vanillic acid supplementation on stress response, emotionality, and visuospatial memory. *Behavioural brain research*, *412*, 113403.

Mouchaileh, N., & Hughes, A. J. (2020). Pharmacological management of Parkinson's disease in older people. *Journal of Pharmacy Practice and Research*, *50*(5), 445-454.

Murray, M. M., & Antonakis, J. (2019). An introductory guide to organizational neuroscience. *Organizational Research Methods*, *22*(1), 6-16.

Nagappan, P. G., Chen, H., & Wang, D. Y. (2020). Neuroregeneration and plasticity: a review of the physiological mechanisms for achieving functional recovery postinjury. *Military Medical Research*, *7*(1), 30.

National Research Council (2011). Environment, housing, and management. *In Guide for the Care and Use of Laboratory Animals. 8th edition*. The National Academies Press: Washington, DC, 246.

Nwozo, O. S., Effiong, E. M., Aja, P. M., & Awuchi, C. G. (2023). Antioxidant, phytochemical, and therapeutic properties of medicinal plants: A review. *International Journal of Food Properties*, *26*(1), 359-388.

Nyman, N. (1959). Determination of glutathione peroxidase in tissue. *Analytical Biochemistry*, 28, 481.

Obeng, S. K., Kulhánek, M., Balík, J., Černý, J., & Sedlář, O. (2024). Manganese: from soil to human health—a comprehensive overview of its biological and environmental significance. *Nutrients*, *16*(20), 3455.

Ohiagu, F. O., Chikezie, P. C., Ahaneku, C. C., & Chikezie, C. M. (2022). Human exposure to heavy metals: toxicity mechanisms and health implications. *Material Science & Engineering International Journal*, *6*(2), 78-87.

Olufunmilayo, E. O., Gerke-Duncan, M. B., & Holsinger, R. D. (2023). Oxidative stress and antioxidants in neurodegenerative disorders. *Antioxidants*, *12*(2), 517.

Pajarillo, E., Nyarko-Danquah, I., Digman, A., Multani, H. K., Kim, S., Gaspard, P., Aschner, M., & Lee, E. (2022). Mechanisms of manganese-induced neurotoxicity and the pursuit of neurotherapeutic strategies. *Frontiers in pharmacology*, *13*, 1011947.

Poeppel, D., and Adolfi, F. (2020). Against the Epistemological Primacy of the Hardware: The Brain from Inside Out, Turned Upside Down. eNeuro, 7(4), ENEURO.0215-20.2020.

Prakash, S., & Verma, S. (2024). Harnessing the Therapeutic Potential of Plant-Derived Natural Products in Neurological Disorders. *Journal of Drug Discovery and Health Sciences*, *1*(01), 28-33.

Pyatha, S., Kim, H., Lee, D., & Kim, K. (2022). Association between heavy metal exposure and Parkinson's disease: a review of the mechanisms related to oxidative stress. *Antioxidants*, *11*(12), 2467.

Rakoczy, K., Szlasa, W., Saczko, J., & Kulbacka, J. (2021). Therapeutic role of vanillin receptors in cancer. *Advances in Clinical and Experimental Medicine*, *30*(12), 1293-1301.

Ramadoss, D. P., & Sivalingam, N. (2020). Vanillin extracted from Proso and Barnyard millets induce apoptotic cell death in HT-29 human colon cancer cell line. *Nutrition and Cancer*, *72*(8), 1422-1437.

Ray, S., & Gaudet, R. (2023). Structures and coordination chemistry of transporters involved in manganese and iron homeostasis. *Biochemical Society Transactions*, *51*(3), 897-923.

Roland, P. E. (2023). How far neuroscience is from understanding brains. *Frontiers in Systems Neuroscience*, *17*, 1147896.

Rost, N. S., Brodtmann, A., Pase, M. P., van Veluw, S. J., Biffi, A., Duering, M., Hinman, J.D., & Dichgans, M. (2022). Post-stroke cognitive impairment and dementia. *Circulation research*, *130*(8), 1252-1271.

Roy, T., Pal, N., & Das, N. (2024). Biochemical, Biosynthetic and Biotechnological Approaches for an Orchid-Derived Natural Flavoring and Therapeutic Agent Vanillin-A Review. *The Chemistry inside Spices & Herbs: Research and Development: Volume 3*, 66-108.

Sabina, M., Zakhrokhon, T., & Gulamovna, D. B. (2024). Nervous System and Its Main Functions. *Eurasian Journal of Medical and Natural Sciences*, *4*(1-1), 61-67.

Sahana, S., Sarkar, J., Mandal, S., Chatterjee, I., Dhar, S., Datta, S., & Mondal, S. (2025). Multi-omics approaches: transforming the landscape of natural product isolation. *Functional & Integrative Genomics*, *25*(1), 132.

Salam, M. A., Al-Amin, M. Y., Salam, M. T., Pawar, J. S., Akhter, N., Rabaan, A. A., & Alqumber, M. A. (2023, July). Antimicrobial resistance: a growing serious threat for global public health. In *Healthcare* (Vol. 11, No. 13, p. 1946). MDPI.

Salau, V. F., & Islam, M. S. (2024). Vanillin: a natural phenolic compound with neuroprotective benefits. In *Natural Molecules in Neuroprotection and Neurotoxicity* (pp. 1857-1879). Academic Press.

Sanders, A. P., Claus Henn, B., & Wright, R. O. (2015). Perinatal and childhood exposure to cadmium, manganese, and metal mixtures and effects on cognition and behavior: a review of recent literature. *Current environmental health reports*, *2*(3), 284-294.

Santiago, R.M., Barbieiro, J., Lima, M.M., Dombrowski, P.A., Andreatini, R. and Vital, M.A., 2010. Depressive-like behaviors alterations induced by intranigral MPTP, 6-OHDA, LPS and rotenone models of Parkinson's disease are predominantly associated with serotonin and dopamine. *Progress in Neuro-Psychopharmacology and Biological Psychiatry*, 34(6), 1104-1114.

Sathish, T., Parusharamudu, M., & Manjari, P. S. (2021). OXIDATION OF VANILLIN BY IODATE IN AQUEOUS ACETIC ACID MEDIUM: A KINETIC AND MECHANISTIC STUDY. *Journal of Advanced Scientific Research*, *12*(04), 220-226.

Schmahmann, J. D. (2019). The cerebellum and cognition. Neuroscience letters, 688, 62-75.

Scipioni, M., Kay, G., Megson, I., & Lin, P. K. T. (2018). Novel vanillin derivatives: Synthesis, anti-oxidant, DNA and cellular protection properties. *European journal of medicinal chemistry*, *143*, 745-754.

Serreli, G., & Deiana, M. (2023). Role of dietary polyphenols in the activity and expression of nitric oxide synthases: A review. *Antioxidants*, *12*(1), 147.

Sharifi, S. A., Zaeimdar, M., Jozi, S. A., & Hejazi, R. (2023). Effects of soil, water and air pollution with heavy metal ions around lead and zinc mining and processing factories. *Water, Air, & Soil Pollution*, *234*(12), 760.

Smolyaninova, L. V., Timoshina, Y. A., Berezhnoy, D. S., Fedorova, T. N., Mikheev, I. V., Seregina, I. F., & Dobretsov, M. G. (2023). Impact of manganese accumulation on Na, K-ATPase expression and function in the cerebellum and striatum of C57Bl/6 mice. *Neurotoxicology*, *98*, 86-97.

Sobańska, Z., Roszak, J., Kowalczyk, K., & Stępnik, M. (2021). Applications and biological activity of nanoparticles of manganese and manganese oxides in in vitro and in vivo models. *Nanomaterials*, *11*(5), 1084.

Sokolov, A. A., Miall, R. C., and Ivry, R. B. (2017). The cerebellum: adaptive prediction for movement and cognition. Trends in cognitive sciences, 21(5), 313-332.

Spence, C. (2022). Odour hedonics and the ubiquitous appeal of vanilla. *Nature Food*, *3*(10), 837-846.

Srivastava, A., Srivastava, P., Pandey, A., Khanna, V. K., & Pant, A. B. (2019). Phytomedicine: A potential alternative medicine in controlling neurological disorders. In *New look to phytomedicine* (pp. 625-655). Academic Press.

Studer, J. M., Schweer, W. P., Gabler, N. K., & Ross, J. W. (2022). Functions of manganese in reproduction. *Animal Reproduction Science*, *238*, 106924.

Sumayya, A. S., & Muraleedhara Kurup, G. (2021). In vitro anti-inflammatory potential of marine macromolecules cross-linked bio-composite scaffold on LPS stimulated RAW 264.7 macrophage cells for cartilage tissue engineering applications. *Journal of Biomaterials Science, Polymer Edition*, *32*(8), 1040-1056.

Sun, Q., Li, Y., Shi, L., Hussain, R., Mehmood, K., Tang, Z., & Zhang, H. (2022). Heavy metals induced mitochondrial dysfunction in animals: Molecular mechanism of toxicity. *Toxicology*, *469*, 153136.

Tarnacka, B., Jopowicz, A., & Maślińska, M. (2021). Copper, iron, and manganese toxicity in neuropsychiatric conditions. *International journal of molecular sciences*, *22*(15), 7820.

Tazon, A. W., Awwad, F., Meddeb-Mouelhi, F., & Desgagné-Penix, I. (2024). Biotechnological advances in vanillin production: from natural vanilla to metabolic engineering platforms. *BioChem*, *4*(4), 323-349.

Wang, J., An, W., Wang, Z., Zhao, Y., Han, B., Tao, H., Wang, J., & Wang, X. (2024). Vanillin has potent antibacterial, antioxidant, and anti-inflammatory activities in vitro and in mouse colitis induced by multidrug-resistant Escherichia coli. *Antioxidants*, *13*(12), 1544.

Wang, L., Huang, J., Liu, Z., & Wang, C. (2025). Decoding the Secrets of Odor-Active Compounds in Dark Tea. *Comprehensive Reviews in Food Science and Food Safety*, *24*(3), e70206.

Wei, N., & Guan, Z. Z. (2021). Damage in nervous system. In *Coal-burning Type of Endemic Fluorosis: Pathophysiology and Clinical Treatments* (pp. 105-124). Singapore: Springer Singapore.

Wen, J. J., & Garg, N. J. (2018). Manganese superoxide dismutase deficiency exacerbates the mitochondrial ROS production and oxidative damage in Chagas disease. *PLoS neglected tropical diseases*, *12*(7), e0006687.

Xiang, Y., Wang, L., Wei, Y., Zhang, H., & Emu, Q. (2022). Excessive manganese alters serum biochemical indices, induces histopathological alterations, and activates apoptosis in liver and cerebrum of Jianzhou Da'er goat (Capra hircus). *Comparative Biochemistry and Physiology Part C: Toxicology & Pharmacology*, *252*, 109241.

Xu, J. (2022). Assessing global fungal threats to humans. *MLife*, *1*(3), 223-240.

Yang, J., Chen, Y. Z., Yu-Xuan, W., Tao, L., Zhang, Y. D., Wang, S. R., Zhang, G.C., & Zhang, J. (2021). Inhibitory effects and mechanisms of vanillin on gray mold and black rot of cherry tomatoes. *Pesticide Biochemistry and Physiology*, *175*, 104859.

Yu, S. P., Jiang, M. Q., Shim, S. S., Pourkhodadad, S., & Wei, L. (2023). Extrasynaptic NMDA receptors in acute and chronic excitotoxicity: implications for preventive treatments of ischemic stroke and late-ons*et al*zheimer's disease. *Molecular Neurodegeneration*, *18*(1), 43.